DISSERTATION ZUR ERLANGUNG DES DOKTORGRADES

DER FAKULTÄT FÜR BIOLOGIE

DER LUDWIG-MAXIMILIANS-UNIVERSITÄT MÜNCHEN

Functional Analysis of Epstein-Barr Virus microRNAs Early After Infection of Human Primary B Lymphocytes

Takanobu Tagawa

Submitted on September 30th, 2015.

Accepted at the oral examination on May 17th, 2016.

Primary examiner: Prof. Dr. Dirk Eick

Secondary examiner: Prof. Dr. Heinrich Leonhardt

ERKLÄRUNG

Hiermit erkläre ich, dass die vorliegende Arbeit mit dem Titel

„Functional Analysis of Epstein-Barr Virus microRNAs Early After Infection of Human Primary B Lymphocytes“

von mir selbstständig und ohne unerlaubte Hilfsmittel angefertigt wurde, und ich mich dabei nur der ausdrücklich bezeichneten Quellen und Hilfsmittel bedient habe. Die Arbeit wurde weder in der jetzigen noch in einer abgewandelten Form einer anderen Prüfungskommission vorgelegt.

München, September 30th 2015

Takanobu Tagawa

Table of Contents

Abstract

Epstein-Barr virus (EBV), a member of the human herpes virus family, encodes 44 micro RNAs (miRNAs). Several reports demonstrated their pro-proliferative and anti-apoptotic functions, but very few cellular targets of viral miRNAs are known and the physiological functions of these miRNAs are largely elusive.

To identify important target genes of EBV-encoded miRNAs, I infected primary human B lymphocytes and systematically studied the effects of the viral miRNAs in the cells early after infection. Transcriptome and protein analyses of EBV-infected B cells showed that viral miRNAs down-regulated not only pro-apoptotic genes like *PMAIP1*, as expected, but also genes with dedicated functions in immunity including cytokines such as IL-12 and IL-6, MHC molecules, several co-stimulatory receptors, and B cell signaling-related genes like Fc receptors. Using luciferase reporter assays, I found that EBV miRNAs could directly repress the *PMAIP1* gene and *IL12B*, a gene coding for a subunit of the IL-12 cytokine, via their 3'-UTRs. In particular, multiple EBV miRNAs target *IL12B* suggesting that viral miRNAs regulate certain cellular transcripts robustly, redundantly, and perhaps cooperatively.

As EBV miRNAs appeared to control a multitude of immune-regulatory genes, I investigated several immunological phenotypes. Reduced IL-12 secretion led to a suppression of Th1 differentiation in co-culture assays with EBV-infected B cells, indicating an immune evasive function of viral miRNAs. Moreover, EBV miRNAs down-regulated antigen presentation by MHC class II and interfered with $CD4^+$ effector T cell responses including IFN-γ secretion and cytotoxicity. Taken together, EBV-encoded miRNAs globally disrupt multiple functions of the adaptive immune system early after infection and thus protect EBV-infected B cells from antiviral immune responses of the human host.

Introduction

Human microRNAs

MicroRNAs (miRNAs) are small RNA molecules of ~22 nucleotides in length (Bartel, 2004). Generally, miRNAs such as hsa-miR-155 originate from dedicated miRNA genes whereas other miRNAs stem from introns of protein-encoding transcripts or snoRNAs (Ha and Kim, 2014). Transcribed RNAs are processed by Drosha RNase to short-hairpin RNAs ("primary miRNA") in the nucleus, are transported to the cytosol, processed by Dicer RNase to double-stranded RNAs ("pre-mature miRNA"), and form complexes, termed RNA-Induced Silencing Complex (RISC), as single-stranded RNAs ("mature miRNA") with other proteins like Argonaute (Bartel, 2004). Human cells encode four different Argonaute genes (*AGO1* to *AGO4*). The gene products of the *AGO* genes all bind to miRNA molecules without a clear preference (Landthaler et al., 2008). Among them, AGO2 is the only member of the AGO family with an endonuclease activity ("Slicer" activity) and directly cleaves bound mRNAs (Ha and Kim, 2014). RISCs, which contain miRNAs mainly bind to the 3'-UTRs of target mRNAs depending on the complementarity between miRNAs and mRNAs (Bartel, 2009; Agarwal et al., 2015). Binding to RISC represses translation followed by mRNA degradation in most cases (Djuranovic et al., 2012; Selbach et al., 2008). One of the mechanisms that causes the translational repression prior to mRNA degradation is the localization of RISC-mRNA to P-bodies, which results in the isolation of mRNAs from the translational machinery (Fig. 1; Liu et al., 2005a; 2005b).

There are several features unique to the gene regulatory mechanism of miRNAs: (i) since target recognition by miRNAs canonically depends on 6 to 8 nucleotides in the miRNAs (the "seed" sequence; Agarwal et al., 2015), a single miRNA species can potentially target hundreds of mRNAs simultaneously (Bartel, 2004); (ii) the repressive strength of miRNAs is limited compared with conventional transcriptional factors and termed the "fine-tuning" ability of miRNAs (Sevignani et al., 2006; Selbach et al., 2008); (iii) in the minority of cases, miRNAs down-regulate genes at protein but not at transcript levels (Fig. 1; Selbach et al., 2008); (iv) a single miRNA occupies very little genomic space such that multiple miRNAs often form clusters in the human genome. For example, the mir-17-92 cluster contains six independent miRNAs in a single transcript, hence miRNAs in this cluster will be expressed at the same time in a polycistronic manner (Olive et al., 2013).

The significance of miRNAs has become apparent during the last decade and it is now well accepted that they mediate important functions in cells of all vertebrates regulating and fine-tuning many cellular processes including development, tumorigenesis, and immune responses (Schickel et al., 2008; Xiao and Rajewsky, 2009).

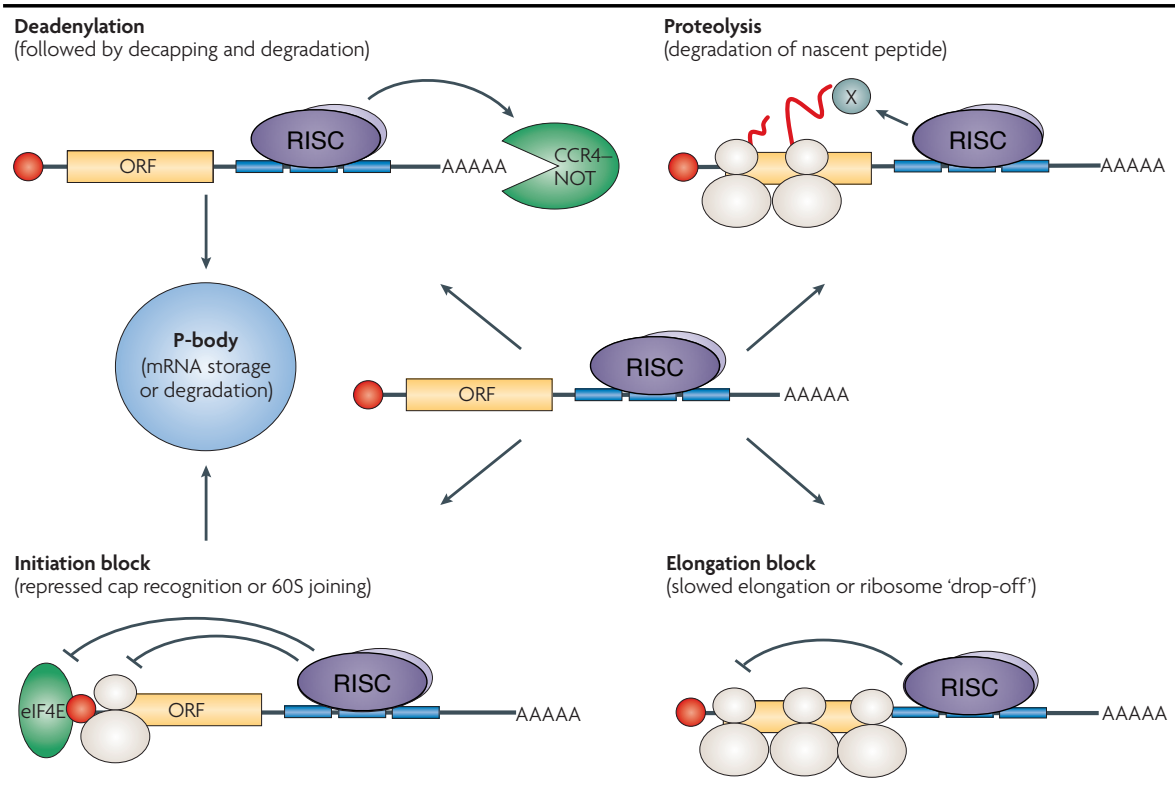

(modified from Filipowitcz et al., 2007)

Figure 1 Proposed mechanisms of miRNA-mediated translational gene repression
miRNA-containing RNA-induced silencing complex (RISC) mainly bind to 3'-UTRs of target mRNAs and induce translational repression through various mechanisms. Only the deadenylation of mRNAs leads to accelerated degradation of mRNAs, suggesting that the regulation by miRNAs results in the reduction of protein levels but not necessarily in the reduction of transcript levels.

EBV-encoded miRNAs

miRNAs encoded by herpes viruses are reported to play important roles in cell proliferation, development, immune regulation, and other processes in infected cells (Grundhoff and Sullivan, 2011; Skalsky and Cullen, 2010). Epstein-Barr Virus (EBV) was found to encode a total of 44 mature miRNAs (Fig. 2; Cai et al., 2006; Pfeffer et al., 2005; Qiu et al., 2011), which, even among herpes viruses, is a very high number. The functions of these miRNAs encoded by EBV (EBV-encoded miRNAs or EBV miRNAs) have been mostly elusive because these miRNAs do not bear similarities to miRNAs of other herpes viruses or

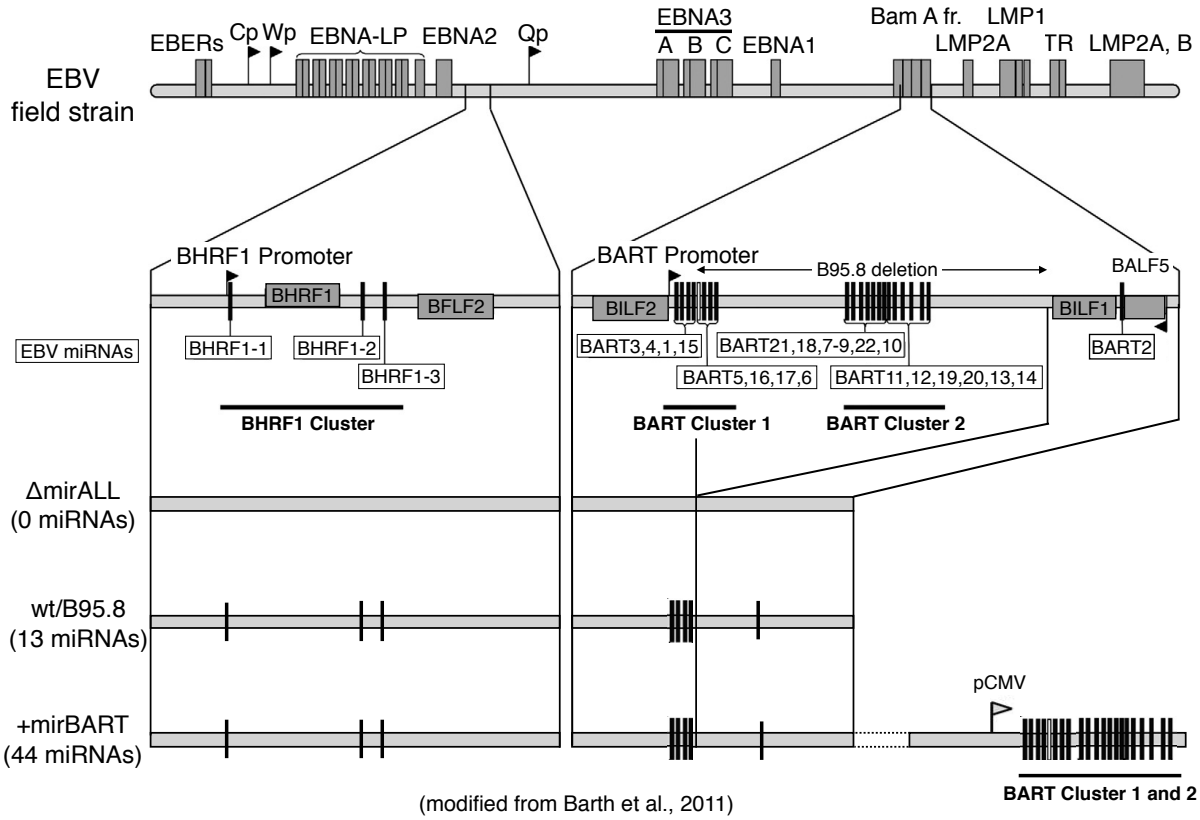

Figure 2 Genomic locations of EBV-encoded miRNAs and EBV strains used in this work
Field strains of EBV contain 44 mature miRNAs. miRNAs are encoded in three clusters (BHRF1 cluster, BART cluster 1, BART cluster 2) and in a single locus for miR-BART2. In this work, three EBV strains, ΔmirALL (no miRNAs), wt/B95.8 (wt; 13 miRNAs), and +mirBART (44 miRNAs) EBV were used. wt/B95.8 EBV is based on the laboratory strain B95.8, which contains a deletion in the BART cluster region. +mirBART EBV was cloned to restore the miRNAs within the B95.8 deletion by cloning all the miRNAs of the BART clusters under control of the CMV promoter and introducing into wt/B95.8 EBV (Seto et al., 2010). ΔmirALL EBV was established by mutating all the miRNA-coding loci such that the corresponding regions of transcripts would have no short-hairpin structures, which are necessary to the biogenesis of miRNAs (Seto et al., 2010).

of the vertebrate cells (Walz et al., 2009). This situation makes it difficult to deduce the physiological functions of EBV miRNAs from better-studied miRNAs. As a counter-example, Kaposi sarcoma-associated herpes virus (KSHV) encodes miR-K12-11, which is an orthologue of hsa-miR-155 and miR-K12-11 shares the same target transcripts of miR-155 (Dahlke et al., 2012; Gottwein et al., 2007).

The majority of EBV-encoded miRNAs is encoded in three main clusters, the BHRF1 cluster, the BART cluster 1, and the BART cluster 2 (Fig. 2; Barth et al., 2011). An exception is a single miR-BART2, which is distantly encoded from any of the three miRNA-encoding clusters of EBV. These viral miRNAs are expressed in most EBV-infected B cells but, depending on the latency type, the expression levels of the three miRNA-containing transcripts may differ (Cai et al., 2006; Qiu et al., 2011). In the early phase after infection,

during the so-called pre-latent phase, all known miRNAs encoded by EBV are expressed (Seto et al., 2010). Therefore, it is conceivable that EBV miRNAs implement important regulatory functions during the pre-latent phase.

Anti-apoptotic and pro-proliferative functions of EBV miRNAs

Previously, our former colleague Eri Seto and other groups have demonstrated that a cluster of EBV miRNAs, the BHRF1 cluster, has significant anti-apoptotic and pro-proliferative cellular functions early after infection of primary human B cells (Feederle et al., 2011a; 2011b; Seto et al., 2010). Nevertheless, the genes regulated by miRNAs of the BHRF1 cluster that cause these phenotypes are unknown to date (Grundhoff and Sullivan, 2011).

Targets of miRNAs encoded by EBV have been studied by several groups in established EBV-infected cell lines obtained from biopsies of Nasopharyngeal carcinoma (NPC) and Burkitt's lymphoma (BL), or lymphoblastoid cell lines (LCL) derived from infecting primary B lymphocytes with EBV *in vitro* (Barth et al., 2011; Dölken et al., 2010; Erhard et al., 2013; Kuzembayeva et al., 2012; Riley et al., 2012; Skalsky et al., 2012; Vereide et al., 2013). By high-throughput target screens using immunoprecipitation in combination with deep sequencing, the authors have identified many potential targets of EBV miRNAs including pro-apoptotic genes such as *BBC3* (Choy et al., 2008) and *CASP3* (Vereide et al., 2013). None of these reported pro-apoptotic genes, however, were targeted by BHRF1 cluster miRNAs (Barth et al., 2011). In addition, the catalogues of predicted targets published by different groups have a surprisingly small overlap (Klinke et al., 2014), which includes *IPO7*, a well-established target of ebv-miR-BART3 (Dölken et al., 2010; Kuzembayeva et al., 2012; Skalsky et al., 2012; Vereide et al., 2013). The lack of an apparent consensus and the inconsistencies in the published literature (Seto et al., 2010) may be due to profound differences in gene expression patterns between different, long-term cultivated, and EBV-infected cell lines that do not reflect the impact of these viral miRNAs.

EBV and immune evasion early after infection

EBV has developed several strategies to fend off antiviral immune responses of the infected human host. For example, EBV establishes a latent infection in B cells which express only a minimal set of viral genes, a strategy which can be considered as a fundamental mechanism of immune evasion (Ressing et al., 2008). EBV also encodes several immunoevasins that suppress the presentation of viral antigens in the lytic phase during virus synthesis (Hislop et al., 2007; Rowe et al., 2007; Zuo et al., 2009). Moreover, an EBV latent membrane protein controls T cell responses directed against latently infected cells (Rancan et al., 2015).

Despite these measures, EBV antigen-specific effector T cells constitute a considerable fraction of the memory T-cell repertoire of the latently EBV-infected human host (Hislop et al., 2002). Prior to establishing a stable, latent phase, many viral lytic genes are expressed for a short period of time in newly infected B cells during the initial, pre-latent phase, which lasts seven to ten days (Kalla and Hammerschmidt, 2012). Among such genes, at least two immunoevasins of the lytic cycle, BNLF2a and BCRF1 (viral IL-10), are also expressed immediately upon B-cell infection (Jochum et al., 2012). BNLF2a and viral IL-10 interfere with the recognition of infected cells by EBV-specific effector T cells and natural killer cells, respectively, but they are insufficient to abrogate T cell recognition completely (Jochum et al., 2012).

Viral miRNAs and immune evasion

In addition to anti-apoptotic functions, EBV miRNAs also reportedly down-regulate *MICB* (Nachmani et al., 2009), *CXCL11* (Xia et al., 2008), and *NLRP3* (Haneklaus et al., 2012) and thus interfere with innate immune responses and inflammation. Interestingly, *MICB*, a gene coding for a ligand of the activating receptor NKG2D expressed on T and NK cells, is also targeted by miRNAs of KSHV and human cytomegalovirus (Grundhoff and Sullivan, 2011; Nachmani et al., 2009). This result suggests that pathways involved in immune evasion are common targets of miRNAs encoded by herpes viruses (Grundhoff and Sullivan, 2011). For now, the consensus of the field is that viral miRNAs mainly contribute to evade innate immune responses. The only known exception is endoplasmic reticulum aminopeptidatse 1 or ERAP1, a critical component for appropriate antigen presentation via

MHC class I, which was reported to be targeted by a single miRNA in human cytomegalovirus (Blum et al., 2013; Cullen, 2013; Stern-Ginossar et al., 2007).

As discussed in the previous section, the suppression of adaptive immune responses early after infection likely contributes to the success of EBV infection. It is therefore possible that EBV miRNAs play a role in this regard for two reasons: (i) EBV miRNAs are expressed during all stages of infected B cells (Cai et al., 2006; Seto et al., 2010); (ii) miRNAs are non-immunogenic and are unlikely to provoke antiviral cellular responses because they are indistinguishable from human miRNAs.

The aim and the design of my research project

In my doctoral research, I tried to address the following question: "What are the physiological functions of EBV miRNAs early after infection?" I used human B lymphocytes newly infected with different EBV strains as a model of primary infection, performed high-throughput screenings, and made phenotypic assessments (Fig. 3). The EBV strains I employed differ only in the numbers of miRNAs encoded in their genomes (Fig. 2). This model has several advantages and is superior to established latently EBV-infected cell lines as discussed above: (i) I can assess the early days after infection, when the pro-proliferative and anti-apoptotic functions of viral miRNAs are most apparent; (ii) comparing different EBV strains, which differ only in the capacity to express all, certain, or no viral miRNAs, will provides me with phenotypes tightly connected to the functions of EBV miRNAs; (iii) the primary B cells prepared from different donors are heterogeneous but will reflect the spectrum of miRNA-regulated genes beyond the genetic variability of individuals in contrast to established cell lines. These advantages will allow me to identify the most important physiological targets of EBV miRNAs.

In my experimental model, I infected primary human B lymphocytes with three EBV strains differing in their miRNA content and analysed the transcriptomes of infected cells by deep sequencing in the pre-latent phase, five days post infection (Fig. 3). I identified several immune regulatory pathways that are affected by EBV miRNAs, but also genes involved in preventing cellular apoptosis and regulating the cell cycle as expected from previous studies (Feederle et al., 2011a; 2011b; Seto et al., 2010). With several methods, I identified certain selected genes with promising and potentially interesting functions. Among the

identified genes, I validated *IL12B* (an important cytokine) and *PMAIP1* (a relevant pro-apoptotic gene) as direct targets of EBV miRNAs. I also found that viral miRNAs down-regulate key molecules important for T cell interaction and their immune responses against EBV-infected B cells. Moreover, EBV miRNAs repressed the secretion of the cytokine IL-12 from infected B cells, which resulted in the suppression of type 1 helper T cell (Th1) differentiation. Viral miRNAs also controlled epitope presentation to $CD4^+$ T cells and interfered with the activity of antiviral effector T cells.

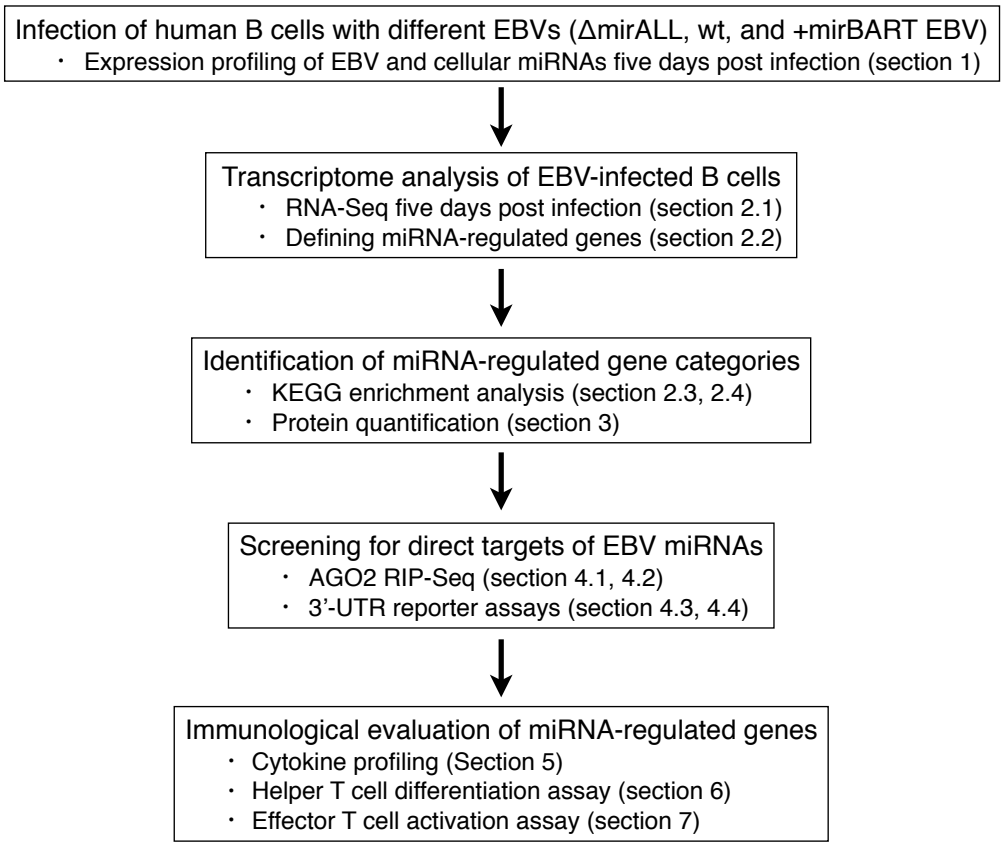

Figure 3 The strategy to decode physiological functions of EBV-encoded miRNAs
I conducted experiments with multiple and sequential steps to identify physiologically important targets and functions of EBV-encoded miRNAs. Corresponding Result sections are indicated for each step.

My findings revealed that EBV-encoded miRNAs govern diverse pathways that regulate B cell proliferation and survival but also critical functions in adaptive immunity, promoting viral immune evasion in the early days of human primary B cells infected with EBV.

Results

1. EBV-infected B cells contain substantial amounts of EBV-encoded miRNAs five days after infection

To investigate the alteration in the transcriptome induced by EBV-encoded miRNAs early after infection, I infected human primary B cells with three EBVs that differ in the number of encoded miRNA. To validate this model of primary infection, I performed miRNA transcriptome analyses and profiled the expression of EBV-encoded miRNAs in B cells infected with the three different EBV strains.

1.1 Infection of primary B cells with EBV mutants with various numbers of miRNAs

I infected primary B cells prepared from adenoids of six donors (Ad1 to Ad6) with three different EBV mutants (Fig. 2, Fig. 4A): wt EBV is based on B95.8, a widely-used laboratory strain of EBV, and contains 13 mature miRNAs (Delecluse et al., 1999); ΔmirALL EBV is devoid of any miRNAs (Seto et al., 2010); +mirBART EBV encodes all 44 mature miRNAs (Seto et al., 2010) listed in miRBase as of 2014 (Kozomara and Griffiths-Jones, 2011). B95.8 strain contains a deletion in miRNA-encoding region (Fig. 2) compared with field wild-type strains, but I call B95.8-based EBV strain as wt EBV for the consistency to the preceding work of Seto et al., 2010.

Previously, we reported that EBV-encoded miRNAs control apoptosis and activate cell cycle progression, two effects that were most apparent five days post infection (Seto et al., 2010). Therefore, I cultivated B cells newly infected with EBV for five days, and performed experiments described in Result section 1.2 and 2 below.

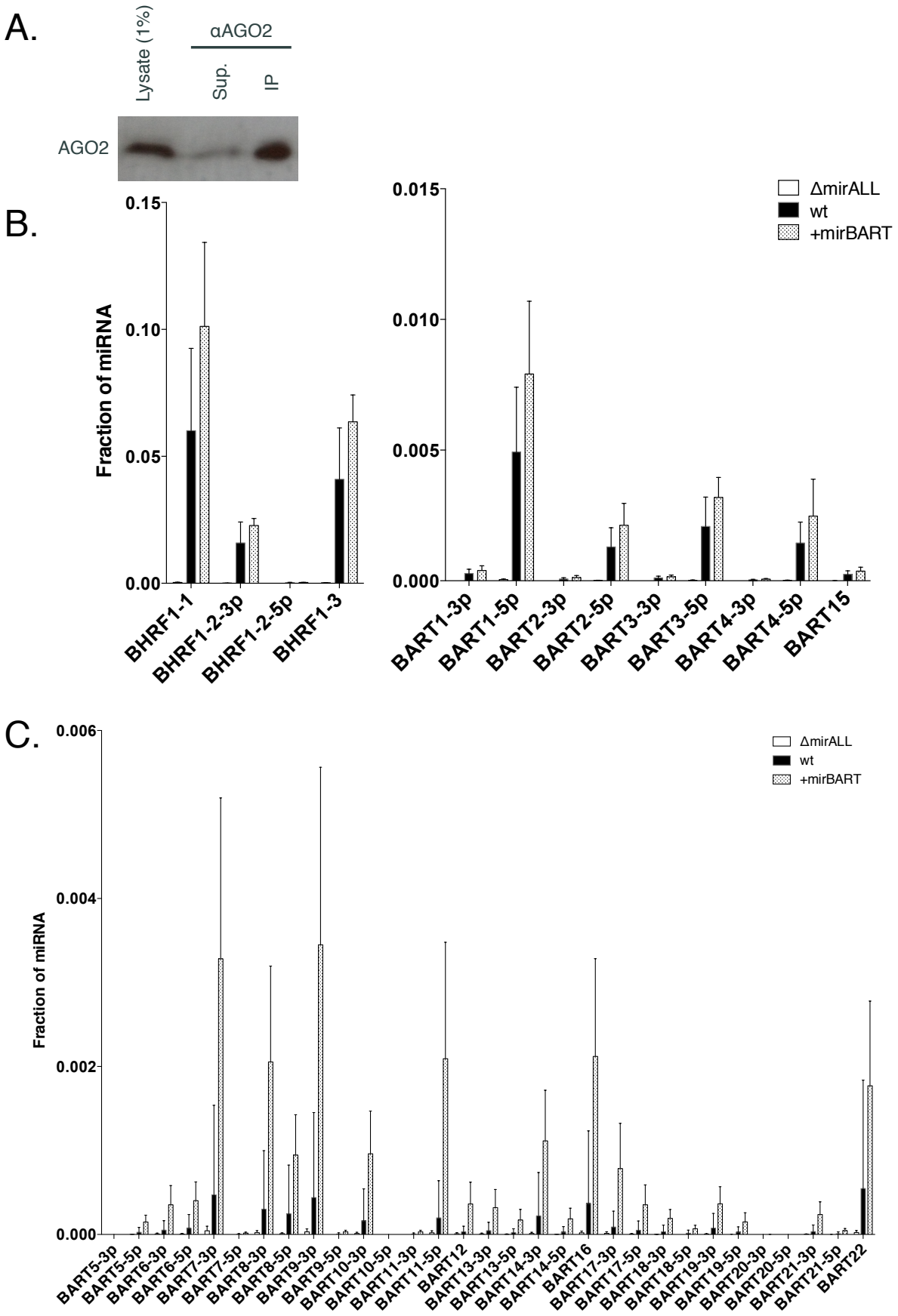

Figure 4 EBV-infected B cells contain EBV-encoded miRNAs early after infection

EBV miRNAs of infected B cells were investigated five days post infection. Primary B cells infected with three EBV strains, ΔmirALL (no miRNAs), wt (13 miRNAs), and +mirBART (44 miRNAs) EBV were

1.2 Relative quantification of EBV-encoded miRNAs in EBV-infected cells

I performed RNA immunoprecipitation and sequencing (RIP-Seq) experiment with an antibody directed against Argonaute2 (AGO2), a core protein of the RISC (RISC; Bartel, 2004), to measure the amount of each EBV-encoded miRNA as well as human miRNAs (Fig. 4A). AGO2 is one of four human Argonaute proteins, which bind small RNAs including miRNAs (Bartel, 2004; Meister et al., 2004). The resulting RNA fragments of RIP-Seq include miRNAs bound to AGO2 and mRNAs captured by RISC (Rüdel et al., 2008). cDNA libraries of the immunoprecipitated RNAs were synthesized by a commercial supplier (vertis Biotechnologie AG). The following deep sequencing was performed by The University of Wisconsin, Biotechnology Center, DNA Sequencing Facility. Jonathan Hoser and Maximillian Hastreiter (Helmholtz Center Munich, Institute of Bioinformatics and Systems biology) performed the mapping and subsequent bioinformatical analyses.

In cells infected with wt EBV and +mirBART EBV, 14.53% (±2.41% SD) and 22.37% (±6.18% SD) of all miRNAs were of viral origin, respectively (Fig. 5A). In contrast, EBV-encoded miRNAs were barely detected in B cells infected with ΔmirALL EBV as expected indicating that my analysis was not compromised by donor B cells accidentally infected with field strains of EBV (Fig. 4B, C).

---

subjected to AGO2 RIP-Seq. EBV-encoded miRNAs were expressed at five days post infection largely as expected.

(A) Enrichment of AGO2 by RIP with an anti-AGO2 antibody. Representative western blot detection of AGO2 after RNA immunoprecipitation (RIP) is shown. 1% of cell lysate, supernatant after RIP, and dynabeads conjugated with anti-AGO2 antibodies were used. The anti-AGO2 antibody precipitated the majority of AGO2 protein.

(B)(C) Fractions of each EBV-encoded miRNAs are shown as the mean of six donors ± Standard Deviation (SD). All EBV-encoded miRNAs but miR-BART20 were expressed in B cells infected with wt or +mirBART EBV. There were almost no EBV-encoded miRNAs in ΔmirALL EBV-infected cells indicating that B cells from six donors were not accidentally infected with field strains of EBV. (B) miRNAs encoded in both wt and +mirBART EBV (BHRF cluster miRNAs and part of BART cluster miRNAs). (C) miRNAs encoded only in +mirBART EBV (a part of BART cluster miRNAs).

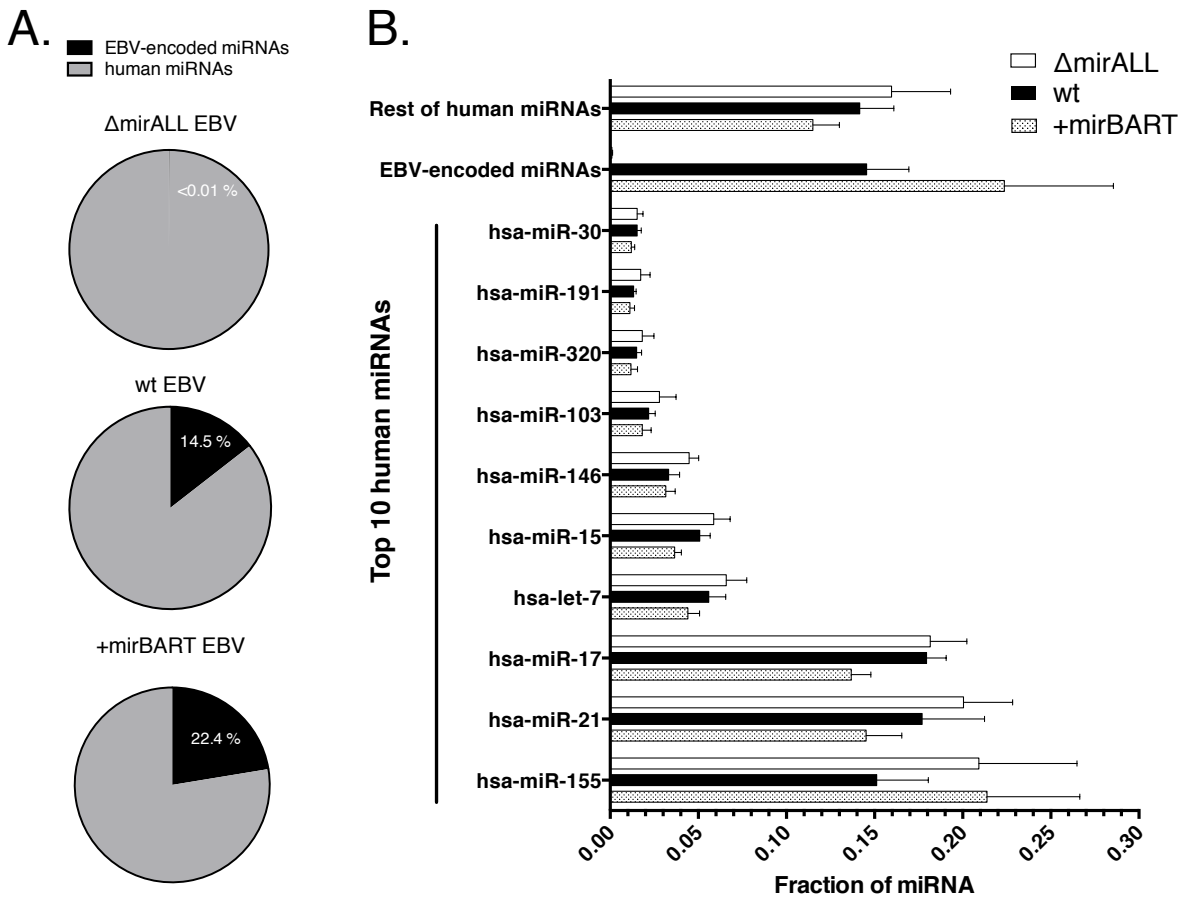

Figure 5 EBV-encoded miRNAs reach sizable fractions of total miRNAs early after infection

miRNA transcriptomes of infected B cells were investigated five days post infection. Human miRNAs were reduced in wt or +mirBART EBV-infected B cells compared with ΔmirALL EBV-infected B cells.

(A) EBV-encoded miRNAs as a fraction of total miRNAs are shown. Means of six donors are presented. +mirBART EBV-infected cells encode more EBV-encoded miRNAs than wt EBV. As a result percentages of miRNAs reflect the number of viral miRNAs encoded by the two EBV strains. In contrast, almost no EBV miRNAs are found in ΔmirALL EBV-infected B cells.

(B) Fractions of the top ten most abundant human miRNAs in infected B cells. As EBV-encoded miRNAs increase, the fractions of the top human miRNAs and the rest of human miRNAs decrease. An exception is miR-155, which increases in +mirBART EBV-infected B cells. Means of six donors ± SD are shown.

1.3 Differential expression of hsa-miR-155 in B cells infected with different EBV strains

From the same RIP-Seq data described in Result section 1.2, I investigated the alteration of the human miRNA transcriptomes induced by the three different EBV strains (Fig. 5A). In B cells infected with wt EBV or +mirBART EBV, the fraction of viral miRNAs increased to substantial levels (14.5% vs. 22.4%) while many of the top ten human miRNAs decreased. This effect was expected because EBV-encoded miRNA were expressed in addition to human miRNAs.

The exception, however, is one of the most abundant human miRNAs in infected B cells, hsa-miR-155, which showed a different expression pattern. The fraction of miR-155 sharply declined in wt compared with ΔmirALL EBV-infected B cells (Fig. 5B). Paradoxically, the fraction of miR-155 in B cells infected with ΔmirALL and +mirBART EBV were almost identical. This observation suggests that viral miRNAs encoded only by +mirBART EBV indirectly caused unexpected strong up-regulation of miR-155 (Fig. 5B, Fig. 2).

2. EBV miRNAs mainly regulate genes involved in immune regulatory pathways, cell proliferation, and the B cell receptor signaling pathway

I analysed the transcriptomic changes induced by EBV miRNAs comparing mRNA transcriptomes obtained by RNA sequencing (RNA-Seq) from ΔmirALL, wt, or +mirBART EBV-infected B cells. Since the transcriptomes and effects of viral miRNAs varied considerably among the six donors, we employed a fold-change based rank score (see Materials & Methods) to define consistently and differentially regulated genes by EBV miRNAs.

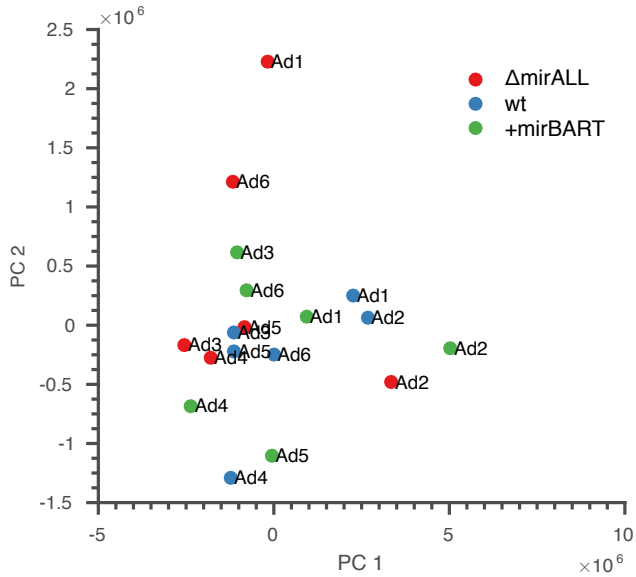

Figure 6 Transcriptomes between primary B cells differ substantially among the six donors
Primary Component Analysis of transcriptomes in six B cells infected with the three EBV strains. First and second primary components (PC1 and PC2) of each donor and virus strain were compared. There was no clear clustering either by donor or by virus strain indicating that infection with the three different viruses did not lead to substantially different gene expression profiles beyond those of the individual B cells from six different donors.

2.1 Summarization and visualization of the transcriptomic data

We applied the Primary Component Analysis (PCA) to eighteen samples (six donors infected with one of the three EBVs) to measure the variability of mRNA transcriptome data among donors and viruses used for infection (Fig. 6). There was no apparent clustering with respect to EBV strains or B cell samples prepared from the six donors. This finding indicated that the transcriptomes between different donors varied too much for EBV miRNAs effects to dominate.

2.2 Comparison of differentially regulated genes

Different donors infected with the same EBV strain cannot be treated as biological replicates due to the individual variations as discussed in Result section 2.1. Therefore, we performed donor-wise comparative transcriptome analyses of B cells infected with the three different EBVs. From these six pairs of data sets based on the infected B cells prepared from six donors, I calculated a fold-change based rank score of each gene, which evaluates the consistency and degree of differential expression among all donors (see Materials & Methods). Using this score, I sorted the identified genes and selected the most strongly and consistently up- or down- regulated genes (Fig. 7A) as candidate targets of EBV miRNAs. As a result, 748, 933, or 913 genes out of 44681 genes (Ensembl Annotations Release 77), which were expressed in EBV-infected B cells, were selected as top down-regulated genes comparing “wt vs. ΔmirALL” EBV-infected B cells, “+mirBART vs. ΔmirALL” EBV-infected B, or “+mirBART vs. wt” EBV-infected B cells, respectively (Fig. 7A, B).

From these directly or indirectly miRNA-targeting genes, I tried to identify canonical targets of EBV miRNAs, which should locate to the intersections of the three comparisons “wt vs. ΔmirALL”, “+mirBART vs. ΔmirALL”, and “+mirBART vs. wt” (Fig. 7B, Supplementary Table 1). This is because wt and +mirBART EBV encode 13 and 44 miRNAs, respectively, but the 13 miRNA in the wt EBV are part of the 44 miRNAs in +mirBART EBV strain (“wt EBV miRNAs”) and only the remaining 31 miRNAs are unique to +mirBART EBV (“+mirBART EBV-unique miRNAs”; Fig. 2). Therefore, the 136 genes within the intersection of the data sets of “wt vs. ΔmirALL” and “+mirBART vs. ΔmirALL” are considered to be the canonical targets of those wt EBV miRNAs (Fig. 7B, Supplementary Table 1). In fact, this intersection contained *IPO7*, a well known target of miR-BART3 (Dölken et al., 2010), which is encoded by wt EBV. Similarly, +mirBART EBV-unique miRNAs are supposed to target 318 genes within the intersection of “+mirBART vs. wt” and “+mirBART vs. ΔmirALL” (Fig. 7B, Supplementary Table 1). Unexpectedly, *LTB* is the only gene in the overlap between “wt vs. ΔmirALL” and “+mirBART vs. wt” (Fig. 7B), which is down-regulated by miRNAs encoded in wt EBV, and is further down-regulated by +mirBART EBV-unique miRNAs. It thus appears that 13 miRNAs, which wt and +mirBART EBV share, and 31 miRNAs unique in +mirBART EBV mainly regulate different groups of genes.

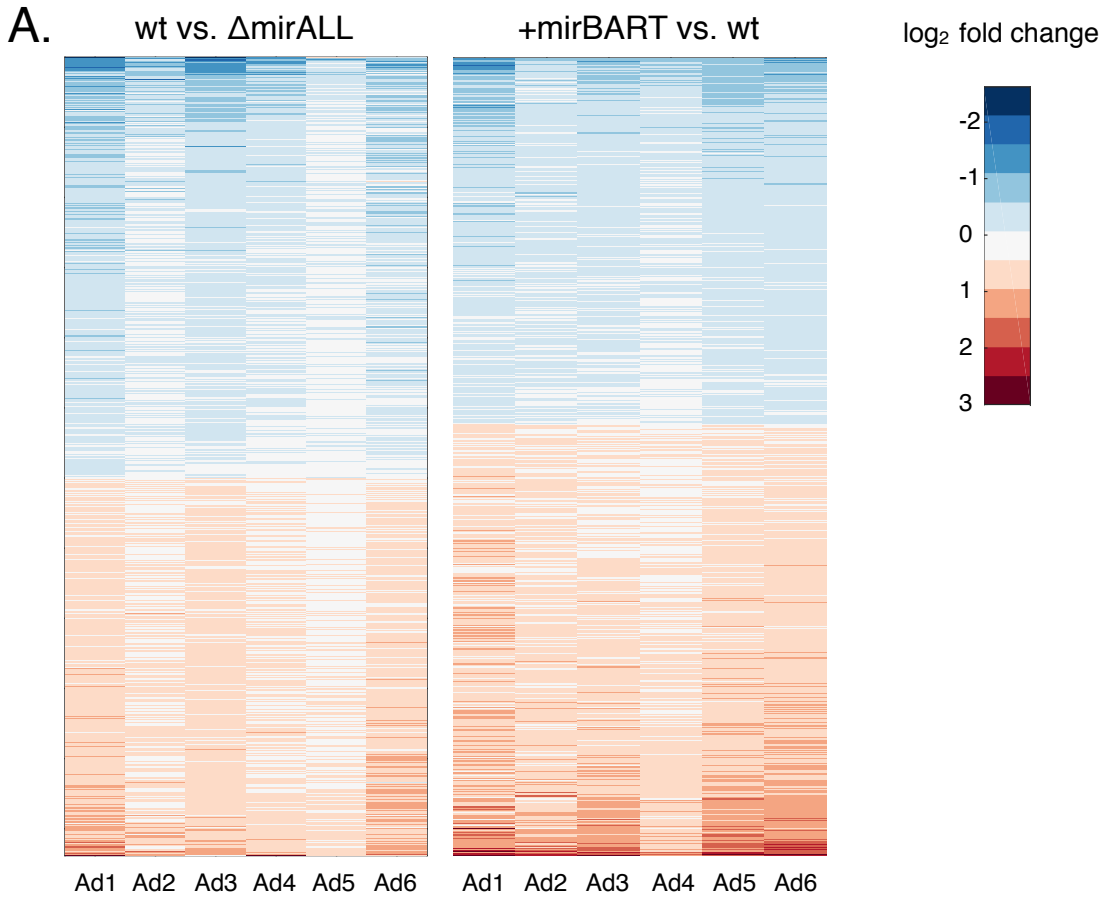

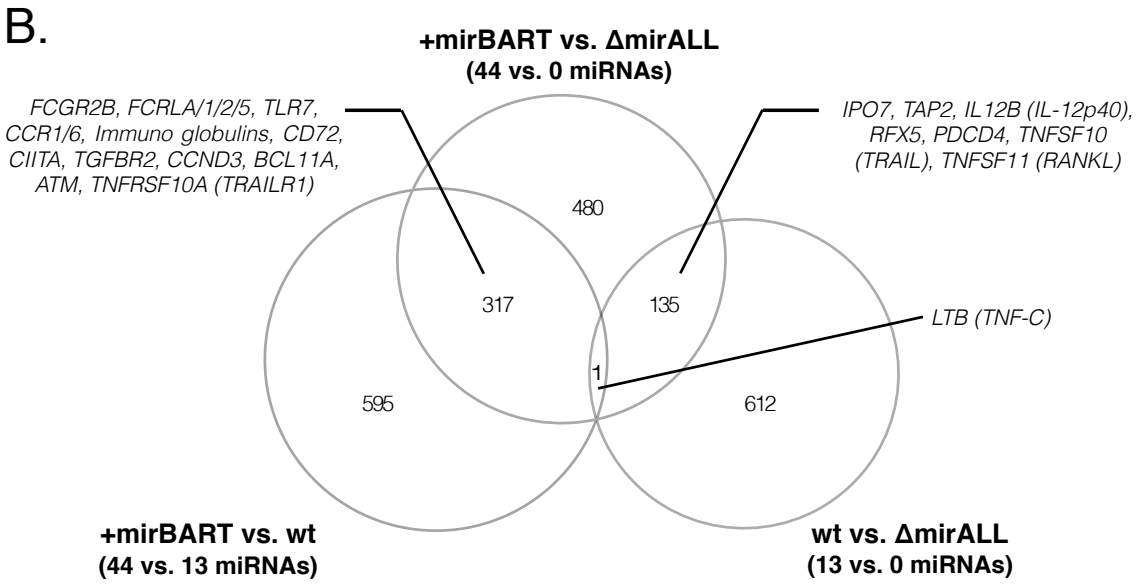

Figure 7 wt EBV miRNAs and +mirBART EBV-unique miRNAs target different cellular genes
Transcriptomes of infected B cells were measured five days post infection. Primary B cells were prepared from six different donors (Ad1 to Ad6), infected with three EBV strains (ΔmirALL, wt, and +mirBART EBV), and subjected to RNA-Seq. miRNAs encoded by wt EBV down-regulated 136 genes including *IPO7*, a known target of an EBV miRNA. +mirBART EBV-unique miRNAs down-regulated 318 genes. Only one gene was commonly repressed by miRNAs encoded by both wt and +mirBART EBV-unique miRNAs suggesting that the two groups of miRNAs mainly regulate different genes.

2.3 KEGG enrichment analysis of genes regulated by miRNAs in wt EBV-infected B cells

To narrow down the presumed functions of EBV miRNAs in the early phase of infection, we analysed the regulation of functional groups of genes according to Kyoto Encyclopedia of Genes and Genomes (KEGG) pathway categories based on the differentially regulated genes discussed in Result section 2.2 (Fig. 8, Supplementary Fig. 1). From the comparison of ΔmirALL and wt EBV-infected B cells, I found that miRNAs encoded in wt EBV regulate genes involved in immune responses and cell proliferation (Fig. 8A). In line with previous findings, pathways linked to apoptosis, cell cycle regulation, and p53 signalling were enriched (Feederle et al., 2011b; Seto et al., 2010; Vereide et al., 2013), and known pro-apoptotic genes (Strasser, 2005) such as *BBC3* (*PUMA*), *PMAIP1* (*NOXA*), and *BAX* were down-regulated at transcript levels (Fig. 8B). Interestingly, regulated pathways included cell adhesion molecules (this KEGG category also encompasses co-stimulatory molecules and HLAs), TNF signaling, antigen processing and presentation, cytokine-cytokine receptor interaction, RIG-I, and Toll-like receptor (TLR) signaling (Fig. 8A).

Affected transcripts in these pathways included cytokines like *IL12B* (coding IL-12p40), *CCL22*, or *TNF* (coding TNF-α), which were among the top candidates of consistently down-regulated transcripts in wt compared with ΔmirALL EBV-infected cells (Fig. 6B). This finding suggested an anti-inflammatory role of EBV miRNAs early after infection. Similarly, transcripts of genes involved in antigen presentation and co-stimulation such as *CD80*, *CD274* (*PDL1*), and *CD40* were consistently down-regulated (Fig. 8B). It thus appears that wt EBV miRNAs control various target genes that may play important roles in immune responses of the infected host directed against EBV-infected primary B cells.

(A) The sorted heatmap displays top differentially expressed transcripts (up- and down-regulated) comparing wt EBV-infected cells versus ΔmirALL EBV-infected cells, or +mirBART EBV-infected cells versus wt EBV-infected cells. Selection was based on a fold change rank score and transcripts with |Z-score|>1.6 are shown (see Materials & Methods). Transcripts are sorted by the fold change rank score and color-coded according to fold changes as indicated.

(B) Overlaps of top down-regulated genes comparing B cells infected with the three EBV strains. The numbers of differentially down-regulated genes (Z>-1.6) and overlaps among them are shown in a pair-wise comparison as indicated. 136 genes within the overlap between "+mirBART vs. ΔmirALL" and "wt vs. ΔmirALL" are likely to be canonical targets of wt EBV miRNAs whereas 318 genes within the overlap between "+mirBART vs. ΔmirALL" and "+mirBART vs. wt" likely encompass main targets of +mirBART EBV-unique miRNAs. In line with this observation, *IPO7*, a well-known target of wt EBV miRNAs, is located in the overlap between "+mirBART vs. ΔmirALL" and "wt vs. ΔmirALL". There was no overlap between "+mirBART vs. wt" and "wt vs. ΔmirALL" except one gene (*LTB*) indicating that the canonical targets of wt EBV miRNAs and +mirBART EBV-unique miRNAs are different. Several genes in the intersections are shown as examples.

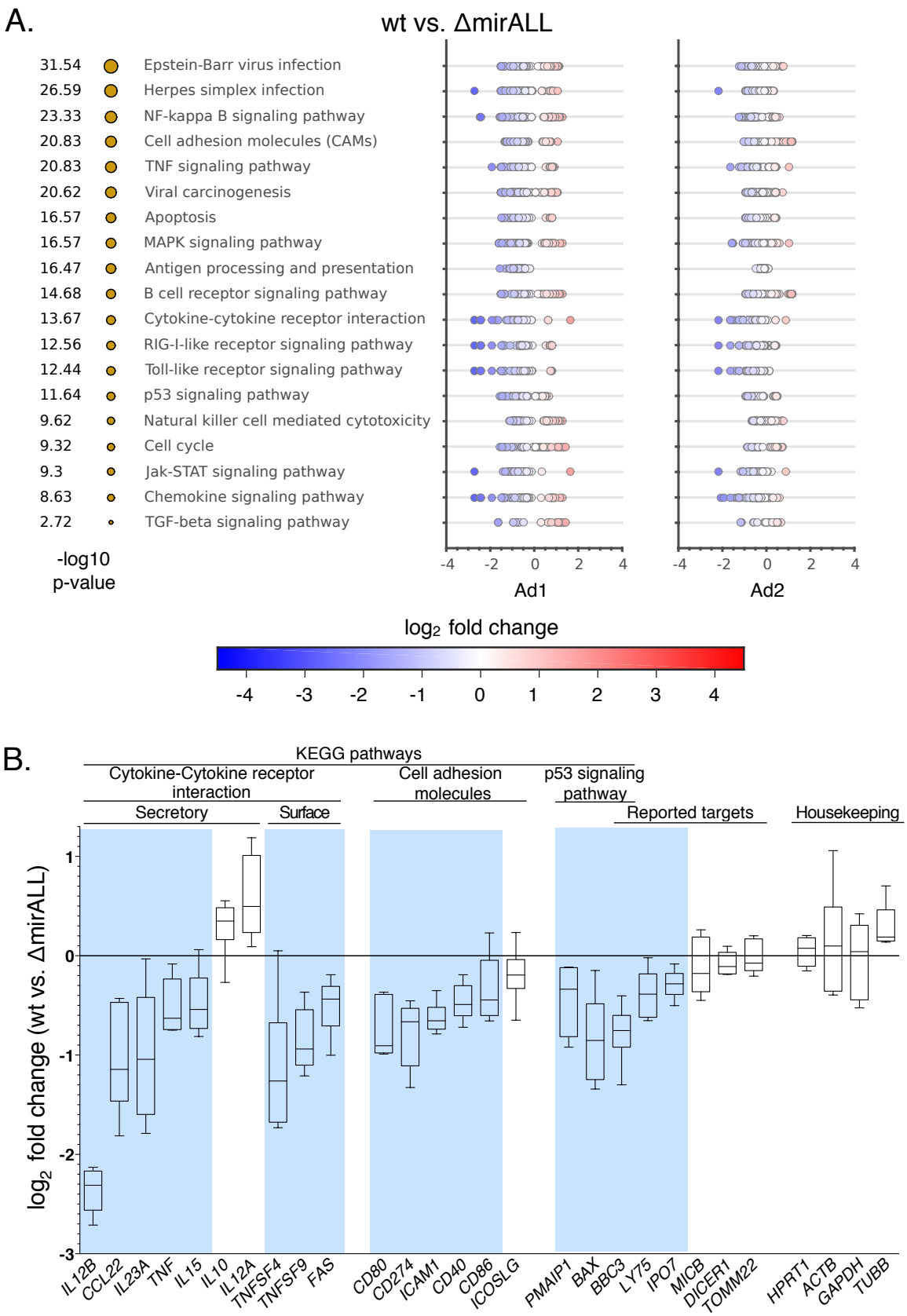

Figure 8 Viral miRNAs in wt EBV mainly regulate genes involved in immune regulatory pathways and cell proliferation

To deduce the physiological functions of EBV miRNAs, a KEGG pathway enrichment analysis was applied with the viral miRNA-regulated genes shown in Fig. 7. I observed that miRNAs of wt EBV regulate genes linked to immune regulatory pathways and cell proliferation.

2.4 KEGG enrichment analysis of genes regulated by miRNAs in +mirBART EBV-infected B cells

As in Result section 2.4, I classified targeted genes regulated by +mirBART EBV-unique miRNAs according to the KEGG pathway categories (Fig. 9, Supplementary Fig. 2). Pathways previously identified in the pair-wise comparison of “wt vs. ΔmirALL” were also enriched comparing “+mirBART vs. wt” EBV-infected B cells with high probabilities (Fig. 8A, Fig. 9A). This finding suggests that +mirBART EBV-unique miRNAs regulate genes in pathways involved in immune responses and cell proliferation as wt EBV miRNAs do. The p-values of the enriched categories that stem from the comparison of “+mirBART vs. wt” are similar to “wt vs. ΔmirALL”, but the fold changes observed in the latter were generally lower (Fig. 8A, Fig. 9A, Supplementary Fig. 1, Supplementary Fig. 2). This tendency may reflect the overall low expression of +mirBART EBV-unique miRNAs compared with miRNAs encoded in wt EBV (Fig. 4B, C). Considering the fact that the overlap between canonical targets of wt EBV miRNAs and +mirBART EBV-unique miRNAs contain just one gene (Result section 2.2; Fig. 7B), my results imply that these two classes of miRNAs regulate the same pathways but different genes.

(A) KEGG enrichment analysis of selected pathways, which are listed according to their significances in descending order. The analysis on the basis of the top differentially regulated genes comparing “wt vs. ΔmirALL” EBV-infected B cells is shown. The sizes of the orange dots indicate -log10 p-value scores. For two of the six donors, fold change values of differentially expressed transcripts are mapped and plotted together with the linked pathways (see Appendix for full data sets). Color codes indicate log2 fold up- or down-regulation (red and blue, respectively) of transcripts as in Fig. 7A. Identified immune regulatory pathways include cytokine-cytokine receptor interaction, the RIG-I-like receptor signaling pathway, and the Toll-like receptor signaling pathway with many down-regulated genes.

(B) Box plots illustrate $\log_2$ fold changes of selected genes, which are targets of miRNAs encoded by wt EBV and associated with adaptive immune responses or the p53 signaling pathway. Many but not all genes in these KEGG pathways are down-regulated in wt compared with ΔmirALL EBV-infected B cell. Genes previously reported to be targets of EBV miRNAs and common housekeeping genes are shown. The blue background shadings indicate top down-regulated genes in “wt vs. ΔmirALL” EBV-infected B cells five days post infection as defined in Fig. 7A.

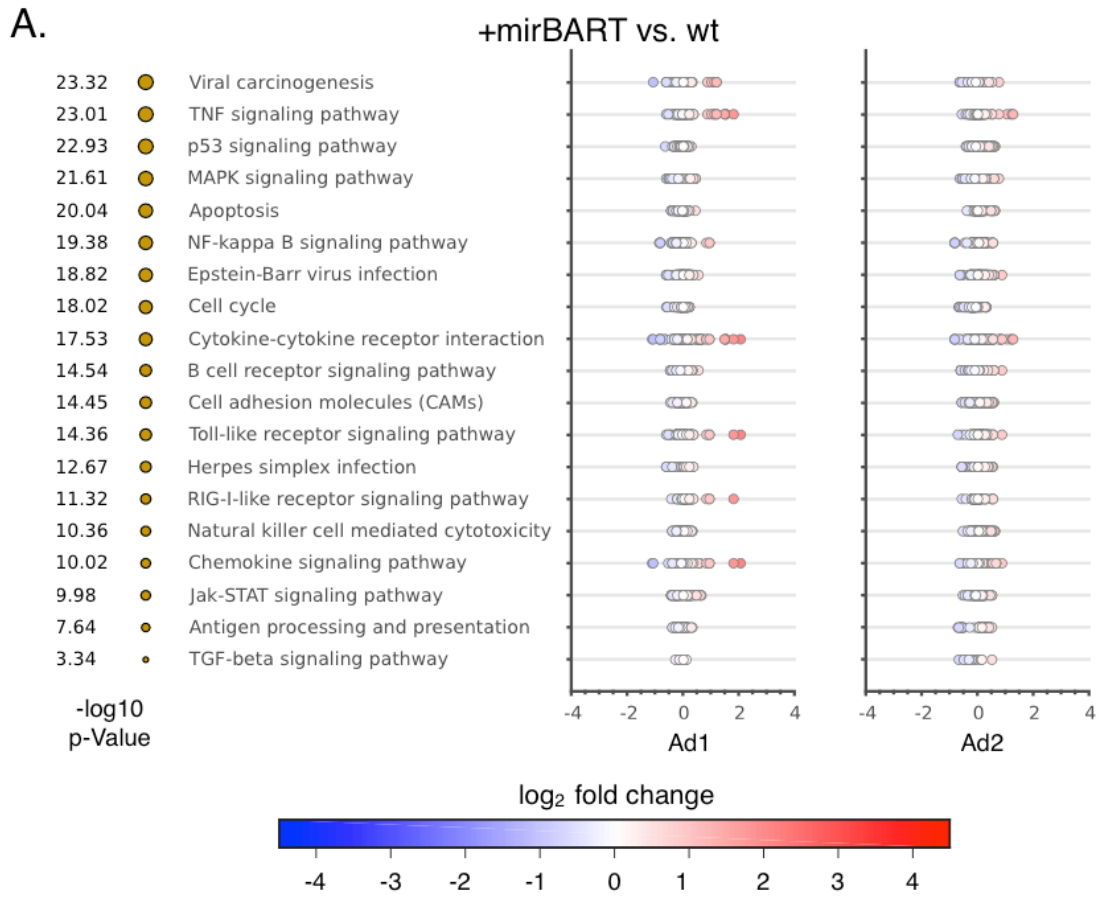

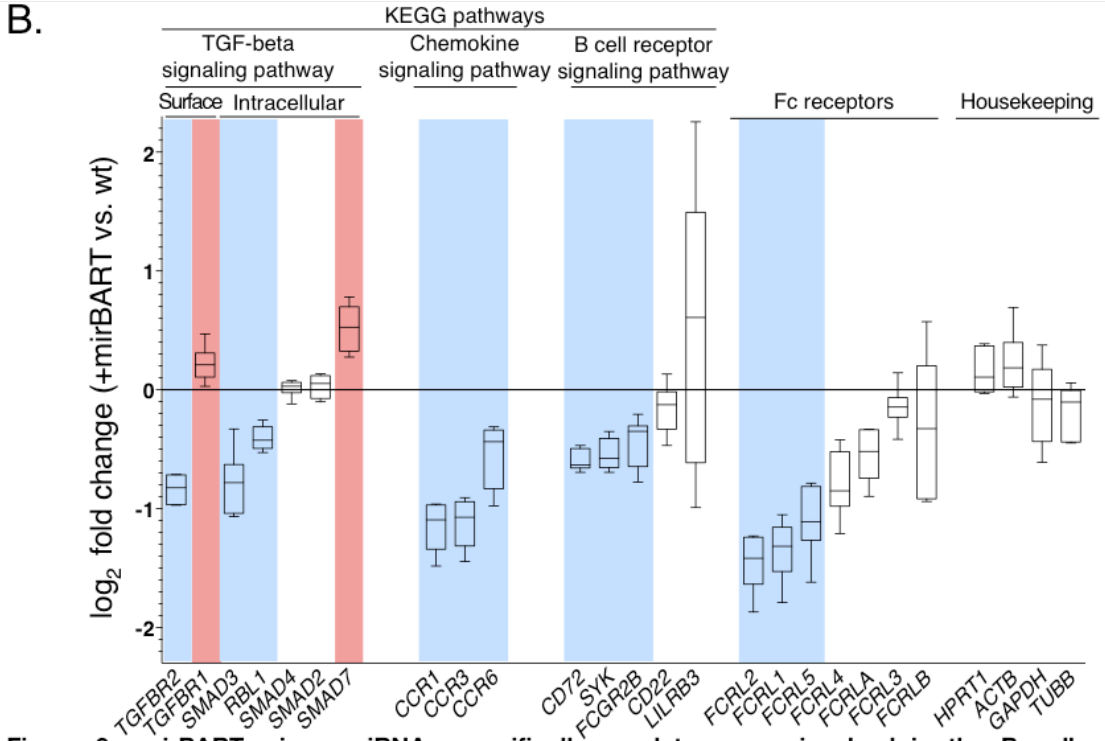

Figure 9 +mirBART-unique miRNAs specifically regulate genes involved in the B cell receptor signaling pathway

A KEGG pathway enrichment analysis was applied with the top regulated genes in +mirBART compared with wt EBV-infected B cells. +mirBART EBV-unique miRNAs control many Fc receptors in addition to immune regulatory pathways or cell proliferation, which appeared in the previous analysis shown in Fig. 8A.

Key molecules in chemokine signaling and TGF-beta signaling such as *TGFBR2* were included in the top down-regulated genes in B cells infected with +mirBART compared with wt EBV (Fig. 9B), but Fc receptor-encoding genes in particular were widely down-regulated at transcript levels (see Fig. 9B with “B cell receptor signaling pathway” and “Fc receptors”). Many products of these down-regulated Fc receptor-encoding genes including *CD72*, *FCGR2B* (*FcγRIIB*), *FCRL2*, *FCRL4*, and *FCRL5* are inhibitory B cell receptor (BCR) co-receptors (Tsubata, 2012), whereas FCRL1 is an activating co-receptor molecule (Leu et al., 2005). Since FCGR2B is known to induce apoptosis upon crosslinking on naive B cells (Tzeng et al., 2005), +mirBART EBV-unique miRNAs may promote a better expansion and survival of EBV-infected B cells by repressing inhibitory BCR co-receptors in a given microenvironment *in vivo*.

(A) KEGG enrichment analysis of selected pathways, which are listed according to their significances in descending order. The analysis on the basis of differentially regulated genes comparing "+mirBART vs. wt" EBV-infected B cells is shown. For two of six donor, transcripts are mapped and plotted together with the linked pathways as in Fig. 8A (see Appendix for full data sets). Generally, the extent of fold change are lower in "+mirBART vs. wt" than in "wt vs. ΔmirALL" EBV-infected B cells, which may be due to the low expression level of +mirBART EBV-unique miRNAs compared with miRNAs encoded by wt EBV (Fig. 4C). The p-values for these pathways are similar comparing differentially regulated genes in "+mirBART vs. wt" and "wt vs. ΔmirALL" EBV-infected B cells suggesting that both miRNAs of wt EBV and +mirBART EBV-unique miRNAs regulate the same pathways but to a different degree.
(B) Box plots illustrate $\log_2$ fold changes of selected genes, which are targets of +mirBART EBV-unique miRNAs and associated with TGF-beta signaling, chemokine signaling, and B cell receptor signaling. The down-regulated genes include many Fc receptors (*FCGR2B*, *FCRLA*, *FCRL1/2/4/5*), which showed consistent down-regulation in +mirBART compared with wt EBV-infected B cells. Common housekeeping genes are shown as well. The blue and red background shadings indicate top down- or up-regulated genes comparing +mirBART versus wt EBV-infected B cells five days post infection as defined in Fig. 7A.

3. Viral miRNA-induced reductions of transcripts correlate with lower protein levels in EBV-infected B cells

I quantified the protein levels of genes whose transcript levels were reduced according to my transcriptome analyses (Result section 2; Fig. 8B, Fig. 9B). I performed ELISAs to quantify the concentrations of released cytokines in cell culture supernatants. I also employed western blot detection and flow cytometry to measure intracellular and cell surface protein levels, respectively (Fig. 10).

IL12B (encoding IL-12p40) was the most strongly and consistently down-regulated gene comparing wt versus ΔmirALL EBV-infected B cells ("wt vs. ΔmirALL"; Fig. 8B). The extent of regulation speaks for a direct role of wt EBV miRNAs in regulating *IL12B*. Since IL12B is a subunit of two cytokines, IL-12 and IL-23 (Szabo al., 2003), I measured the concentration of IL12B in the supernatants of B cells infected either with wt EBV or with ΔmirALL EBV. As a result, the concentration of IL12B is lower in supernatants of wt compared with ΔmirALL EBV-infected B cells at four and eleven days post infection (Fig. 10A).

The pro-apoptotic gene *PMAIP1* was another gene that was consistently down-regulated at the transcript level in wt versus ΔmirALL EBV-infected B cells (Fig. 10B). My colleague Manuel Albanese performed western blot analysis on whole cell lysates from B cells infected either with wt or with ΔmirALL EBV to detect PMAIP1. The protein level of PMAIP1 was reduced in wt EBV-infected B cells compared with ΔmirALL EBV-infected B cells (Fig. 10B), confirming the regulation at the transcript level (Fig. 8B).

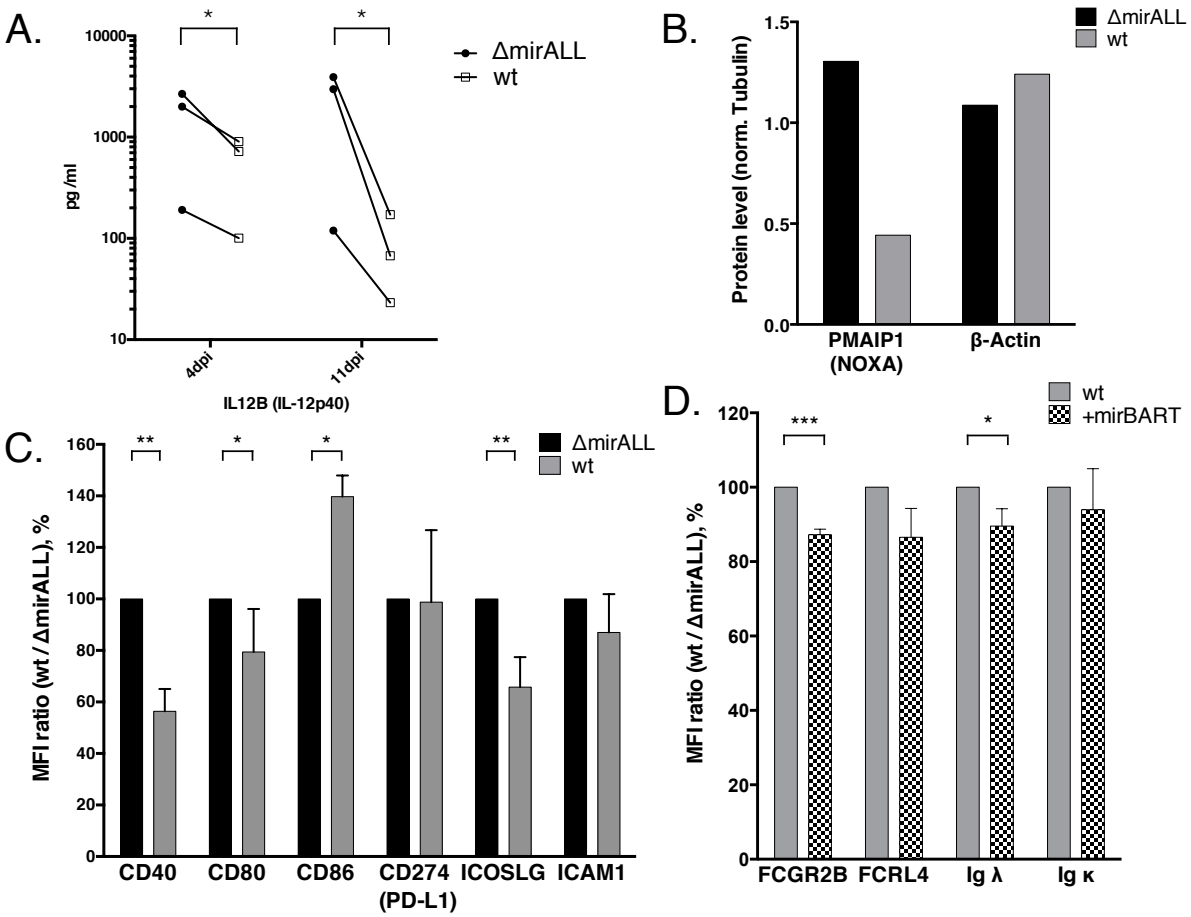

Figure 10 EBV miRNAs regulate steady state protein levels in EBV-infected B cells

I quantified the protein expression of genes that were down-regulated at transcript levels by wt EBV miRNAs or +mirBART EBV-unique miRNAs. For cytokines, intracellular proteins, and cell surface proteins, I employed ELISA, western blotting, and Flow cytometry analysis, respectively. With the exception of certain cell surface proteins, genes that were down-regulated in the transcriptome analysis showed reduced protein levels.

(A) IL12B (IL-12p40) concentrations in supernatants (between four to eight, or 11 to 15 days post infection) from B cells infected with wt or ΔmirALL EBV were measured with ELISA. IL12B secretion was reduced in wt compared with ΔmirALL EBV-infected cells early after infection. Three independent biological replicates are shown. IL12B concentrations were normalized to 1 x 10^6 cells. *: $p<0.05$, two-tailed ratio T test.

(B) Steady state protein levels were investigated by western blot detection using cell lysates from ΔmirALL and wt EBV-infected cells five days post infection. PMAIP1 was down-regulated in cells infected with wt compared with ΔmirALL EBV early after infection. The signal of PMAIP1 and β-Actin (an internal reference gene) are normalized to the signal of Tubulin.

(C)(D) Quantification of cell surface protein levels of genes differentially regulated by viral miRNAs. Primary B cells were infected with wt or ΔmirALL EBV, immunostained, and flow cytometry analysis was performed prior to infection and five days post infection using antibodies directed against the indicated gene products. *: $p<0.05$, **: $p<0.01$, ***: $p<0.001$ of two-tailed ratio T test. Means of three to five biological replicates are shown with SD. (C) wt EBV-infected cells showed down-regulated cell surface expression levels of many immune synapse-related proteins. Ratios of Median Fluorescence Intensity (MFI) of wt versus ΔmirALL infected cells are shown as percentage. Manuel Albanese performed the analysis. (D) +mirBART EBV-unique miRNAs down-regulate cell surface expression levels of Fc receptors and immune globulins. Ratios of MFI (+mirBART versus wt infected cells) are shown as percentage. I performed the analysis.

Lastly, we performed immunostainings followed by flow cytometry analysis to quantify the amounts of several cell surface proteins encoded by genes identified to be top down-regulated genes by EBV miRNAs (Fig. 8B, Fig. 9B). At five days post infection, the majority of these miRNA-targeted targets including CD40, CD80, ICOSLG, and ICAM1 showed reduced surface protein levels on wt compared with ΔmirALL EBV-infected B cells (Fig. 8B, Fig. 10B). Similarly, protein levels of FCGR2B and the immuno globulin light chain lambda, but not kappa, were reduced on the cell surface of +mirBART compared with wt EBV-infected B cells (Fig. 9B, Fig. 10B).

These findings indicate that reduced transcript levels corresponded to lower protein levels in general. The few exceptions speak for unknown mechanisms, which are regulated by EBV miRNAs and indirectly control the levels of functional proteins in EBV-infected B cells.

4. EBV miRNAs redundantly and robustly repress targeted mRNAs

A high-throughput screening like my transcriptome analysis requires a subsequent independent validation to confirm the findings. Here I employed various methods to prove, re-evaluate, and refine direct targets of EBV miRNAs. The transcriptome analysis provided me with information about mRNA reduction by viral miRNAs, but mRNA levels can be regulated directly or indirectly. I performed AGO2 RIP-Seq not only to identify the catalogues of RISC-incorporated miRNAs (Result section 1) but also to find transcripts directly bound by EBV miRNAs. Combining this information with my transcriptome analysis, I performed an efficient screening of the direct targets of viral miRNAs. I also employed luciferase reporter assays for the final validation of transcripts directly repressed by EBV miRNAs. Here I mainly focused on miRNAs encoded by wt EBV.

4.1 Analysis of AGO2 RIP-Seq using IPO7 as a positive control

AGO2 RIP enriches not only miRNAs but also targeted mRNAs (Meister et al., 2004), which are trapped in the RISC to be degraded, eventually. To evaluate whether my RIP-Seq resulted in an enrichment of reads of mRNAs that EBV miRNAs target, I analysed the 3'-UTR of *IPO7* (Fig. 11 top panel), a well-established target of ebv-miR-BART3 (Dölken et al., 2010). For the bioinformatical analysis of mapped reads, we defined an enrichment score, which embodies the enrichment of reads comparing wt with ΔmirALL EBV-infected B cells (see Materials & Methods for details). For all six donors tested, the miR-BART3 binding position in the 3'-UTR of the *IPO7* mRNA provided a clear peak with a high enrichment score (Fig. 11 top panel) indicating that the AGO2 RIP-Seq was sensitive enough to capture the differential binding of EBV miRNAs to mRNA molecules.

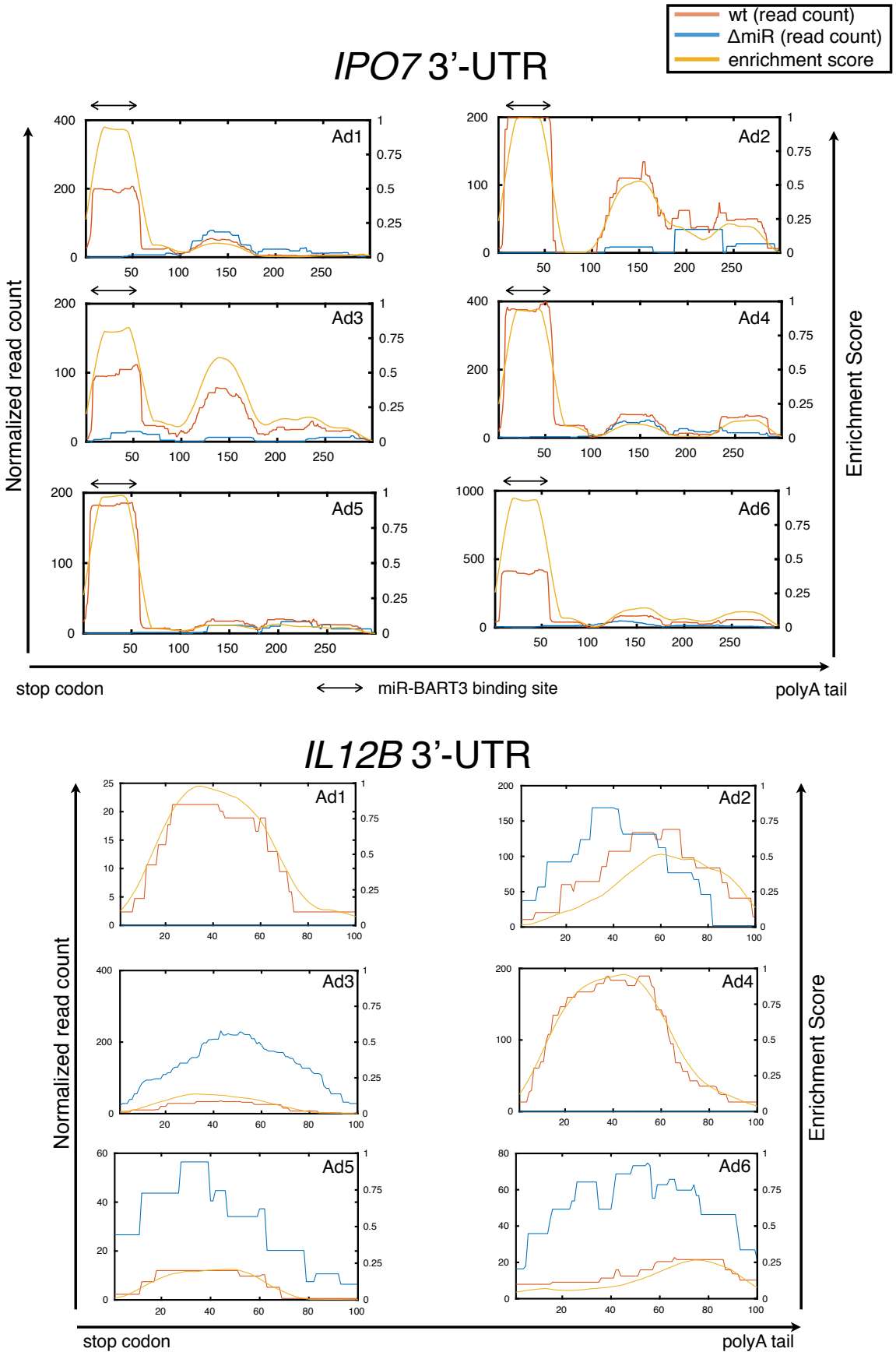

Figure 11 EBV miRNAs bind target mRNAs

AGO2 RIP-Seq analysis of B cells infected with wt EBV or ΔmirALL EBV. EBV-infected B cells were lysed and RIP-Seq against AGO2 was performed five days post infection. Resulting reads were mapped to the

4.2 Prediction of direct targets of EBV miRNAs

To define the threshold levels that likely classify direct targets of EBV miRNAs, I analysed the 3'-UTRs of selected mRNAs of top down-regulated genes according to the transcriptome analysis (Result section 2) and predicted to be direct targets by TargetScan 6 (an *in silico* algorithm to predict direct targets of miRNAs; Garcia et al., 2011). The 3'-UTR of *IL12B* is shown in Fig. 11 (bottom) as an example. *IL12B* was among the most strongly down-regulated gene product regarding transcript and protein levels by wt EBV miRNAs (Fig. 8B, Fig. 10A) and TargetScan predicted that *IL12B* could be directly controlled by ten EBV miRNAs. Still, only donors Ad1 and Ad4 showed a peak with a high enrichment score (Fig. 11). Similarly, the 3'-UTR of the viral miRNA-regulated *PMAIP1* (Fig. 8B, Fig. 10B) showed high enrichment scores only in three infected B cells out of six donors (Supplementary Fig. 3).

From these observations, I decided to select the top read-enriched 3'-UTRs to find transcripts directly bound by EBV miRNAs. We defined the criteria for this purpose as follows: a transcript with a stretch of >20 nucleotides with an enrichment score of >0.6 in its 3'-UTR in two or more donors. In the comparison of "wt vs. ΔmirALL" EBV-infected B cells, 2235 genes including *IPO7*, *IL12B*, *PMAIP1*, *CCL22*, *CD40*, and *FAS*, which were down-regulated at the level of transcript levels (Fig. 8B), fulfilled these criteria (Supplementary Table 2 for the full list of identified genes).

4.3 Luciferase reporter assays with the 3'-UTRs of *IL12B* and *PMAIP1*

Among the candidates discussed in Result section 4.2, I selected *IL12B* and *PMAIP1* to evaluate if they are direct targets of viral EBV miRNAs. I performed luciferase reporter assays with wild-type or mutated 3'-UTRs of *IL12B* and *PMAIP1*. In these assays, miR-BHRF1-2, miR-BART1, or miR-BART2 inhibited the luciferase activity of the *IL12B* reporter (Fig. 12A left). I mutated the predicted binding sites of miR-BART1 or miR-BART2, which

---

human genome (hg19 'core' chromosome-set) and 3'-UTRs of selected genes were examined comparing wt and ΔmirALL EBV-infected B cells. The normalized read enrichment in wt EBV-infected B cells (orange line), +mirBART EBV-infected B cells (blue line), and enrichment scores (yellow line, see Materials & Methods) are shown for all six donors. The presented data were acquired from samples described in Fig. 4.
(Top) The 3'-UTR of *IPO7* mRNA is a well-known target of ebv-miR-BART3 and the enrichment score is very high at the exact binding position of ebv-miR-BART3 in all six samples. This result indicates that the AGO2 RIP-Seq experiments captured the viral miRNA- targeted transcripts.
(Bottom) The 3-'UTR of *IL12B* mRNA is shown. *IL12B* is the strongly down-regulated gene in wt compared with ΔmirALL EBV-infected B cells, but in AGO2 RIP-Seq only two out of six samples had high enrichment scores.

abrogated the ability of miR-BART1 or miR-BART2 to inhibit the *IL12B* reporter (Fig. 12A left, Supplementary Fig. 4) suggesting the direct binding and repression of *IL12B* by viral miRNAs. In addition, miR-BART10 and miR-BART22, which are present in +mirBART EBV but not in wt EBV, directly inhibited the luciferase activity of the *IL12B* 3'-UTR reporter (Fig. 12A left, Supplementary Fig. 4). Mutations of their predicted target sites only partially relieved the inhibition by these miRNAs suggesting the presence of additional unknown binding sites for miR-BART1, -BART10, and –BART22 in the *IL12B* transcript.

Similarly, the *PMAIP1* reporter was directly bound and repressed by miR-BART2 (Fig. 12B right, Supplementary Fig. 4). There are two binding sites for miR-BART2. Mutations of either of these sites abrogated the repressive function of miR-BART2 suggesting that miR-BART2 needs both sites to suppress *PMAIP1* expression fully (Fig. 12B right).

Combining RNA-Seq, AGO2 RIP-Seq, *in silico* prediction, and 3'-UTR reporter assays, I identified a number of miRNAs encoded in wt EBV that directly control the expression of *IL12B* and *PMAIP1*.

4.4 Luciferase reporter assays with 3'-UTRs of *FCGR2B* and *TGFBR2*

I performed 3'-UTR reporter assays with the 3'-UTRs of *FCGR2B* and *TGFBR2* that were among the top down-regulated genes repressed by +mirBART EBV-unique miRNAs (Fig. 12B). I tested the wild-type 3'-UTRs of these transcripts in combination with a number of EBV miRNAs. I selected viral miRNAs that have a 6-mer seed complementarity (Bartel, 2009) as the minimal requirement to be considered. As a result, the *FCGR2B* reporter was inhibited by multiple +mirBART EBV-unique miRNAs (miR-BART7 and miR-BART19), but none of wt EBV miRNAs had an effect (miR-BHRF1-1 and miR-BART2; Fig. 12B). Similarly, different +mirBART EBV-unique miRNAs (miR-BART10 and miR-BART20), but not the wt EBV miRNA miR-BART2, significantly inhibited the luciferase activity of the *TGFBR2* reporter. These findings suggested that several +mirBART EBV-unique miRNAs, but not wt EBV miRNAs, directly repress *FCGR2B* and *TGFBR2* in line with my transcriptome analysis (Result section 2.4; Fig. 7B, Fig. 9B).

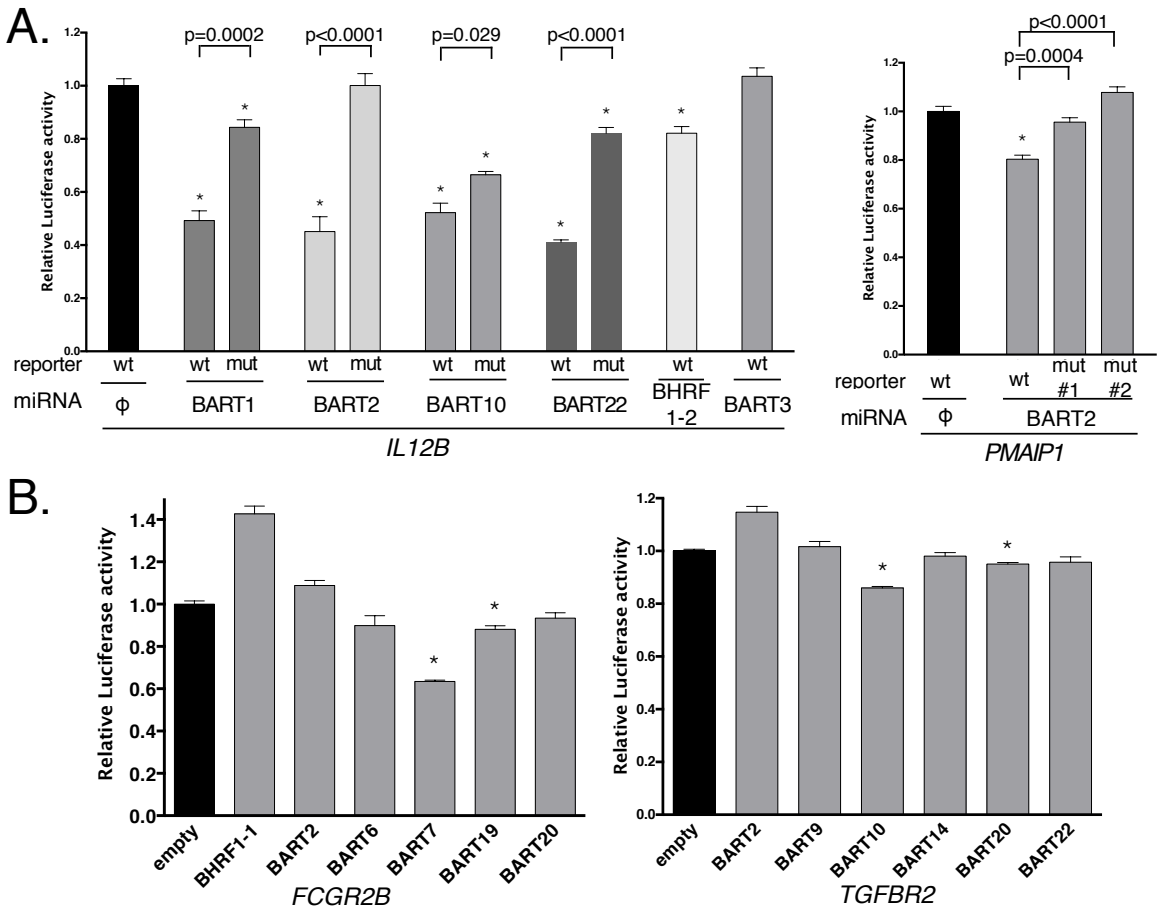

Figure 12 EBV miRNAs redundantly bind and repress target mRNAs

I confirmed *IL12B* and *PMAIP1* as direct targets of EBV miRNAs using luciferase reporter assays. Several viral miRNAs target IL12B redundantly. In addition, I validated *TGFBR2* and *FCGR2B* as targets only of +mirBART EBV-unique miRNAs.

(A) Luciferase reporter assays with 3'-UTRs of *IL12B* or *PMAIP1* and single EBV miRNAs. I performed reporter assays with *IL12B* or *PMAIP1* 3'-UTRs cloned in psiCHECK-2 vectors. These genes were chosen because both *IL12B* and *PMAIP1* were down-regulated in wt compared with ΔmirALL EBV-infected cells (Fig. 8B, 10A, 10B), and AGO2 RIP-Seq showed read enrichment within their 3'-UTRs. The *IL12B* reporter was directly inhibited by five different miRNAs, which include both wt miRNAs and +mirBART EBV-unique miRNAs suggesting a high redundancy of viral miRNAs regulating *IL12B*. The *PMAIP1* reporter was similarly inhibited by one viral miRNA, miR-BART2. ϕ: empty vector, wt: wild-type 3'UTR, mut: 3'-UTR with mutations preventing the binding of EBV miRNAs. *: $p<0.05$, two-tailed unpaired T test for luciferase assay of wt 3'-UTR with empty vector. p-values are shown for the evaluation of mutations as indicated. Means of triplicates ± SD are shown.

(B) Luciferase reporter assays with 3'-UTRs of *FCGR2B* or *TGFBR2*. These genes were repressed in +mirBART compared with wt EBV-infected cells both at transcript and at protein levels (Fig. 9B, 10D). Several +mirBART EBV-unique miRNAs but no wt EBV miRNAs inhibited the 3'-UTR reporters of these genes. *: significant in two-tailed unpaired multiple T test using the Sidak-Bonferroni method of luciferase assay with empty vector. Mean of triplicates ± SD are shown.

5. wt EBV-infected B cells release less pro-inflammatory cytokines than ΔmirALL EBV-infected cell

The KEGG pathway enrichment analysis in the Result section 2.3 showed that cytokines appeared to be among the canonical targets of EBV miRNAs, particularly in wt EBV-infected B cells (Fig. 8). To examine the effects of EBV miRNAs on cytokine secretion from EBV-infected B cells, I closely investigated the regulation of several genes included in the category "Cytokine-Cytokine receptor interaction". I analysed the levels of transcripts and cytokine concentrations with RNA-Seq and ELISA, respectively.

5.1 Transcriptomic profiles of cytokines

Transcript levels of genes encoding pro-inflammatory cytokines like IL-6 (IL6, TNF-α, IL-8, and IL-15), but not the anti-inflammatory cytokine IL-10, in wt EBV-infected B cells were lower compared with ΔmirALL EBV-infected B cells (Fig. 8B, Supplementary Table 1). In addition, cytokines like IL-12 and IL-23, which induce helper T cell (Th) differentiation, were down-regulated in wt compared with ΔmirALL EBV-infected B cells (Fig. 8B). IL-12 and IL-23 are heterodimers that consist of a common subunit IL12B (IL-12p40), which pairs with IL12A (p35) or IL23A (p19), respectively (Szabo al., 2003). Interestingly, *IL12A* was unaffected but both *IL12B* and *IL23A* were down-regulated by wt EBV miRNAs (Fig. 8B). Therefore, the reduced amount of the IL-23 heterodimer (p19/p40) secreted from EBV-infected B cells was expected, but the situation for IL-12 heterodimer (p35/p40) was not obvious.

Taken together, according to the transcriptomic analysis of EBV-infected B cells, miRNAs encoded in wt EBV appeared to interfere with important antiviral immune responses preventing infected cells from producing high levels of pro-inflammatory cytokines and cytokines that promote Th cell differentiation.

5.2 Cytokine profiling by ELISA

I measured the secretion of pro-inflammatory and Th differentiation cytokines as well as an anti-inflammatory cytokine described in Result section 5.1 and asked whether EBV miRNAs control not only mRNA levels but also cytokine secretion. I prepared primary B cells from three different donors and infected them either with wt EBV or with ΔmirALL EBV.

After four or eleven days, I seeded the identical number of cells for each condition in fresh medium, cultivated the cells for four additional days, and quantified the concentration of cytokines in the supernatants with ELISA (Fig. 13). For the detection of the pro-inflammatory cytokines IL-6 and TNF-α, I added CpG DNA, which stimulates TLR9 and enhances the secretion of these cytokines from EBV-infected cells (Iskra et al., 2010). This step was necessary to reliably detect IL-6 and TNF-α. The wt EBV-infected B cells secreted consistently less IL-6 and TNF-α than B cells infected with ΔmirALL EBV. Secretion of IL-12 (p35/p40) and IL-23 (p19/p40), both of which contain the IL12B subunit, were also significantly reduced in wt compared with ΔmirALL EBV-infected cells (Fig. 13 right), even though *IL12A*, which encodes p35, was not down-regulated at the transcript level (Fig. 8B). This finding suggests that IL-12p40, the product of *IL12B* that is strongly controlled by viral miRNAs (Fig. 6B, Fig. 7A, Fig. 8B), was the limiting factor in IL-12 and IL-23 secretion. In contrast to these cytokines, the secretion of the anti-inflammatory cytokine IL-10 showed no clear regulation by viral miRNAs regardless of the addition of CpG DNA (Fig. 13). This result is consistent with my transcriptome analysis (Fig. 8B).

Collectively, ΔmirALL EBV-infected B cells secrete higher amount of several pro-inflammatory cytokines than wt EBV-infected B cells. EBV miRNAs control not only the transcript levels (Result section 5.1) but also the secretion of cellular pro-inflammatory cytokines that may enhance immune responses of the host against EBV-infected B cells. Even further, EBV miRNAs reduce IL-12 and IL-23 secretion, which may result in the suppression of helper T cell differentiation. IL-12 induces the differentiation of naive $CD4^+$ T cells to type 1 helper T cells (Th1 cells), which are known to act against virus-infected cells. It is thus conceivable that EBV benefits from a reduced number of Th1 cells that virus controls via its many viral miRNAs.

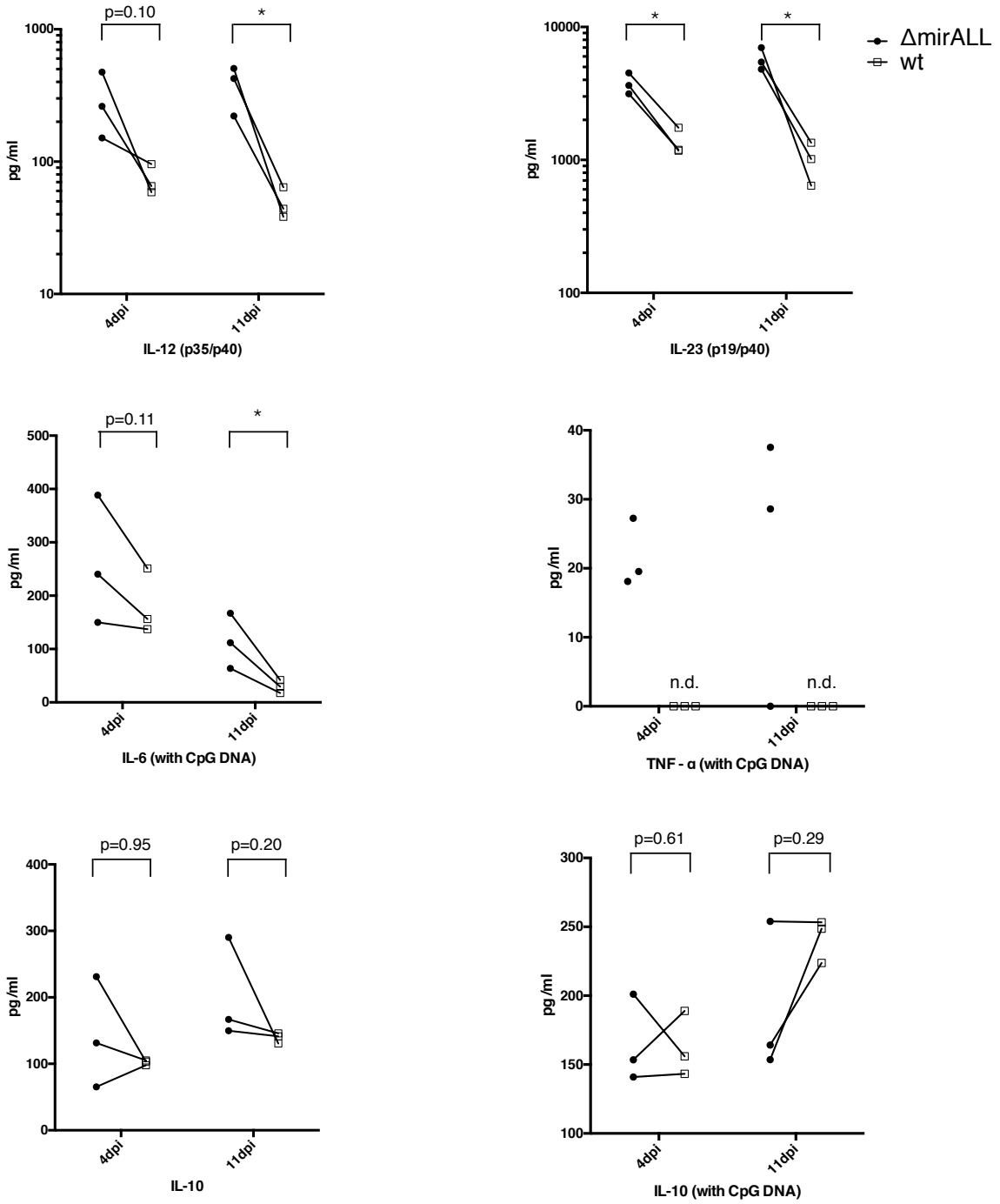

Figure 13 wt EBV-infected B cells secrete less pro-inflammatory cytokines compared with ΔmirALL EBV-infected cells

IL-12, IL-23, IL-6, TNFα, and IL-10 concentrations in supernatants (harvested between 4 to 8, or 11 to 15 days post infection) from B cells infected with wt or ΔmirALL EBV were measured with ELISA. Secretions of the Th differentiation cytokines IL-12 and IL-23, and the pro-inflammatory cytokines IL-6 and TNFα were reduced from wt compared with ΔmirALL EBV-infected cells. In contrast, the secretion of an anti-inflammatory cytokine, IL-10, appeared to be not regulated by viral miRNAs. Three independent biological replicates are shown. The cytokine concentrations were normalized to $1x10^6$ cells. *: $p<0.05$. p-values of two-tailed ratio T test are shown. (Left column) Concentrations of IL-12, IL-23, and IL-10. (Right column) Concentrations of IL-6, TNFα, and IL-10. CpG DNA was added at two time points (4 and 11 days post infection) to induce the secretion of pro-inflammatory cytokines from EBV-infected B cells.

6. Reduced IL-12 secretion from wt EBV-infected B cells interferes with Th1 differentiation of naive CD4$^+$ T cells

The cytokine IL-12 induces the differentiation of naive CD4$^+$ T cells to type 1 helper T cells (Szabo al., 2003), and both its transcript level and secretion are reduced by wt EBV miRNAs (Result section 5). Based on this observation, I hypothesized that the reduced secretion of IL-12 from wt compared with ΔmirALL EBV-infected B cells suppresses Th1 differentiation. To investigate this hypothesis, I employed co-culture experiments.

6.1 Th1 differentiation assay with co-cultured naive CD4$^+$ T cells and infected B cells

I performed co-culture experiments with naive CD4$^+$ T cells and autologous B cells infected with wt or ΔmirALL EBV (Fig. 14) to prove my hypothesis. I proposed that EBV miRNAs repress the secretion of IL-12 from EBV-infected B cells and thereby suppress the differentiation of helper T cells. I sorted naive CD4$^+$ T cells from human donors and stored at -80°C. In parallel, I sorted primary B cells from the same donors, infected them either with wt or with ΔmirALL EBV, and cultivated the two infected cell populations for five days. Naive CD4$^+$ T cells were then thawed, pulsed with CellTrace Violet (to identify stimulated, proliferating cells later), and mixed with EBV-infected B cell in the presence of anti-CD3/anti-CD28 antibodies (to activate T cells and induce their differentiation) for seven days (Fig. 14A). Prior to the analysis, T cells were re-stimulated with PMA/Ionomycin for five hours to induce the secretion of IFN-γ, which is a marker for differentiated Th1 cells. As a result, wt EBV-infected B cells reduced the size of the Th1 population compared with ΔmirALL EBV-infected cells (Fig. 14B, C). T cells cultivated either with ΔmirALL EBV or with wt EBV proliferated equally (Fig. 14B left panel) indicating that EBV miRNAs interfered with Th1 differentiation but did not prevented the proliferation of T cells.

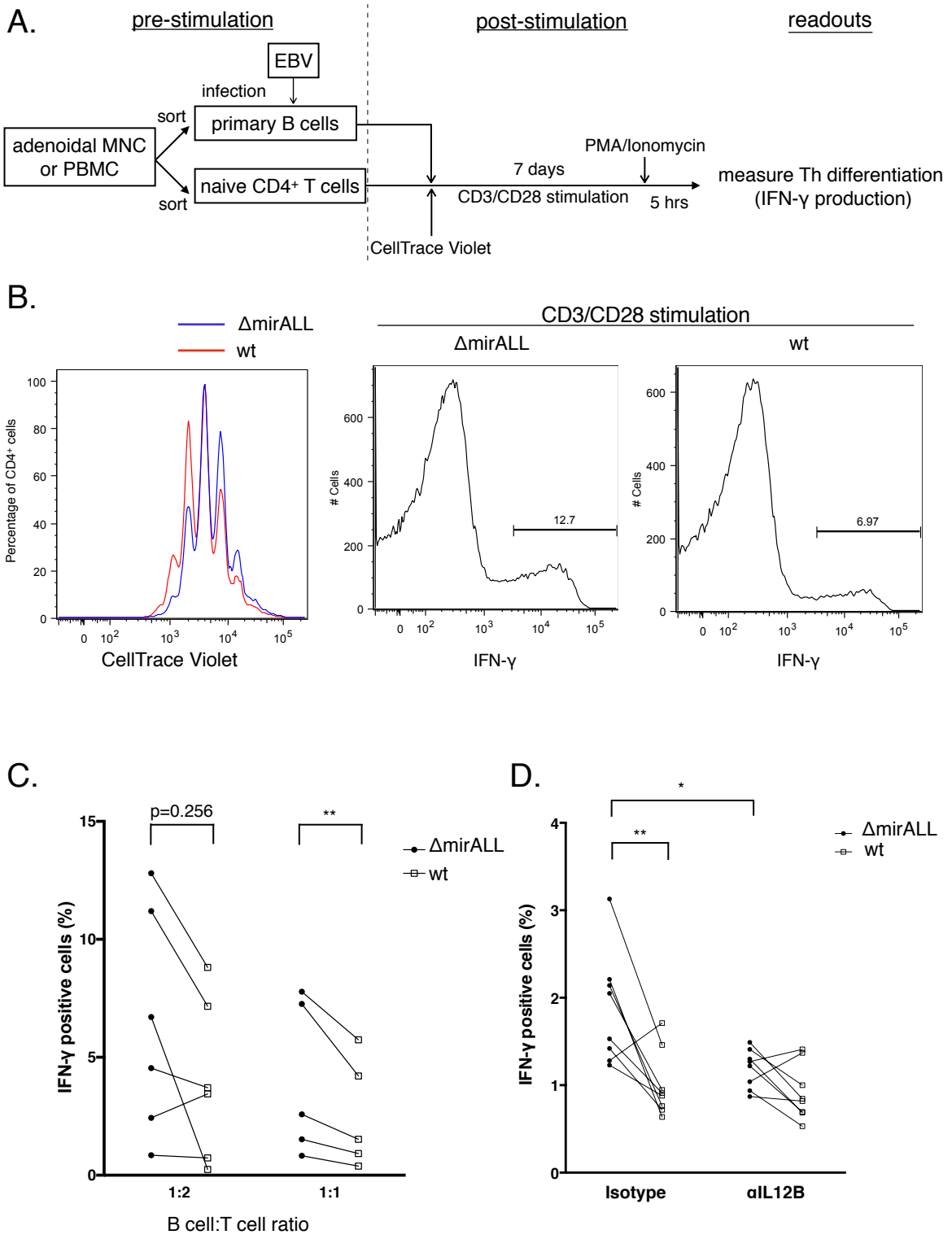

Figure 14 Low IL-12 secretion from wt EBV-infected B cells interferes with Th1 differentiation of naive CD4⁺ T cells

Th1 populations were quantified after co-culture experiments of naive CD4⁺ T cells and infected B cells in an *in vitro* differentiation assay. IL-12 is a key cytokine inducing Th1 differentiation of naive CD4⁺ T cells (Teng et al., 2015). The reduced secretion of IL-12 from wt EBV-infected B cells (Fig. 13) resulted in the reduction of the Th1 population compared with ΔmirALL EBV-infected B cells. T cells cultivated with wt or ΔmirALL EBV-infected B cells proliferated equally under αCD3/αCD28 stimulation.

6.2 Neutralization of IL-12 prevents Th1 differentiation

I performed similar co-culture experiment but used an anti IL12B (IL-12p40) antibody to neutralize the IL-12 cytokine released by wt or ΔmirALL EBV-infected B cells and measured the contribution of IL-12 to Th1 differentiation (Fig. 14D). As an appropriate control, I used an antibody of the same isotype as the IL-12p40 neutralizing antibody. The anti-IL12B antibody, compared with an irrelevant isotype antibody, suppressed Th1 differentiation of T cells co-cultured with ΔmirALL EBV-infected B cells abrogating the difference between wt and ΔmirALL EBV-infected B cells regarding the size of Th1 population (Fig. 14D). This finding indicates that EBV miRNAs interfere with the differentiation of Th1 cells by reducing the secretion of IL-12 from EBV-infected B cells.

(A) Schematic presentation of the Th1 differentiation assay. The naive $CD4^+$ T cells were pulsed with Cell Trace Violet to identify proliferating cells and cultivated for 7 days with autologous B cells that had been infected with EBV five days earlier. αCD3/αCD28 antibodies were added to activate naive $CD4^+$ T cells and to induce their differentiation. T cells were re-stimulated for 5 hours with phorbol 12-myristate 13-acetate (PMA) and ionomycin to induce IFN-γ production prior to immunostaining. Th1 populations of proliferating T cells were quantitated with intracellular IFN-γ staining and flow cytometery analysis.

(B) Th1 populations appeared after the co-culture of naive $CD4^+$ T cells with B cells infected with wt or ΔmirALL EBV. wt EBV-infected B cells reduced the size of the Th1 population compared with ΔmirALL EBV-infected B cells. (Left) A representative flow cytometry analysis of the CellTrace Violet staining of $CD4^+$ T cells after the co-culture with B cells infected with wt or ΔmirALL EBV. T cells cultivated with wt or ΔmirALL EBV-infected B cells proliferated equally under αCD3/αCD28 stimulation. (Right) A representative flow cytometry analysis of intracellular IFN-γ staining after co-cultures of naive $CD4^+$ T cells with B cells infected either with wt or with ΔmirALL EBV. The IFN-γ positive Th1 populations are shown as percentage of proliferating $CD4^+$ T cells.

(C) Statistical analysis of the percentage of IFN-γ positive, proliferating T cells after the co-culture experiment of naive $CD4^+$ T cells with B cells infected either with wt or with ΔmirALL EBV at two different cell ratios as indicated. *: $p<0.05$. p-values of two-tailed ratio T test are shown.

(D) The effect of IL12B neutralization on the fraction of IFN-γ positive T cells in co-cultures with wt or ΔmirALL EBV-infected B cells. B cell:T cell ratio was 1:1. Cytokine neutralization was achieved with 5 µg/ml anti-IL12B (IL-12p40, a subunity of IL-12) antibodies and controls were obtained with an irrelevant antibody of the same isotype. IL12B neutralization abrogated most of the stimulatory effect of ΔmirALL-infected cells on Th1 differentiation. *: $p<0.05$, **: $p<0.01$.

7. EBV miRNAs reduce antigen presentation and suppress recognition of infected B cells by CD4$^+$ T cells

The transcriptome analysis described in Result section 2 revealed that EBV miRNAs regulate genes included in the KEGG pathway "Cell adhesion molecules" that encompasses immunological synapse-related genes. These EBV miRNAs-regulated genes include co-stimulatory molecules, cell adhesion molecules, and MHCs. Down-regulation of these genes will lead to reduced antigen presentation by EBV-infected B cells, hence less recognition by T cells. To evaluate this possibility, Manuel Albanese quantitated protein levels of these gene products on the surface of infected B cells, and determined the activities of effector CD4$^+$ T cells against EBV-infected B cells.

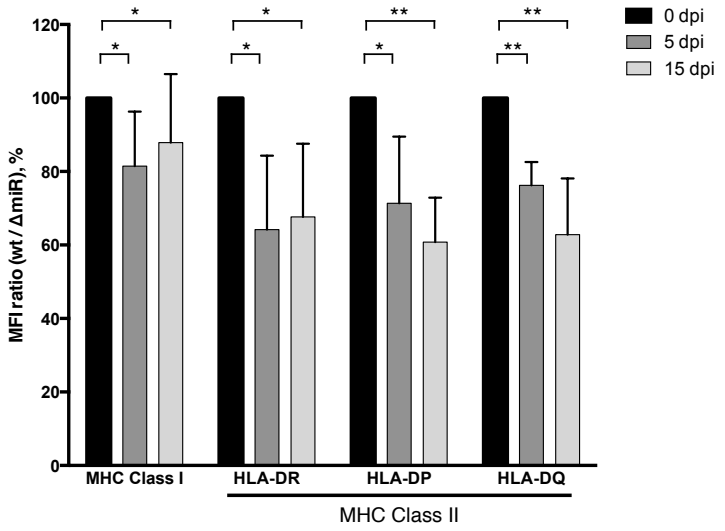

Figure 15 EBV miRNAs reduce antigen presentation by infected B cells

Antigen presentation to effector T cells via MHC class I and II by EBV-infected B cells were assessed by flow cytometry analysis. Ratios of MFI (wt versus ΔmirALL infected cells) of individual HLA molecules prior to infection, five days post infection, or 15 days post infection are shown. wt EBV-infected B cells showed lower protein levels of major MHC class molecules on the cell surface compared with ΔmirALL EBV-infected cells, suggesting a reduced antigen presentation early after infection. *: $p<0.05$, **: $p<0.01$. Means of three to five biological replicates are shown with SD.

7.1 Reduction of MHC molecules, co-stimulatory molecules, and cell adhesion molecules on the surface of infected B cell by EBV miRNAs

For the quantification of antigen presentation, we performed immunostainings of MHC molecules followed by flow cytometry with B cells infected either with wt EBV or with ΔmirALL EBV. At five and 15 days post infection, protein levels of all three major MHC class

II molecules were significantly lower in wt EBV-infected B cells compared with ΔmirALL EBV-infected B cells (Fig. 15) suggesting a reduced antigen presentation to $CD4^+$ T cells. The protein levels of MHC class I molecules were mildly but significantly lower at both time points, too (Fig. 15). These results suggested that, as early as five days post infection, EBV miRNAs in infected B cells may inhibit antigen epitope presentation by both MHC class I and II molecules.

In addition, several, but not all co-stimulatory molecules (CD40, CD80, and ICOSLG) and one cell adhesion molecule (ICAM1) were reduced at cell surface protein levels in wt EBV-infected B cells compared with ΔmirALL EBV-infected B cells (Fig. 10C). Together, these findings support a hypothesis that EBV miRNAs inhibit immune responses of T cells by reducing antigen presentation of EBV-infected B cells. The viral miRNAs control genes including MHC molecules, co-stimulatory molecules, and adhesion molecules necessary for immunological synapse formation.

7.2 Reduced IFN-γ secretion from effector $CD4^+$ T cells upon co-culture with wt EBV-infected B cells

To test the hypothesis stated in Result section 7.1, Albanese expanded $CD4^+$ T cells *ex vivo* by repeated stimulation with an irradiated autologous wt EBV-infected Lymphoblastoid Cell Line (LCL). The expanded EBV-stimulated T cells were incubated with primary B cells, which were infected either with wt EBV or with ΔmirALL EBV and cultivated for five days. For the evaluation of T cell activities, the concentration of secreted IFN-γ was measured of these co-culture experiments after 16 hours (Fig. 16A).

The activity of the LCL-stimulated, EBV antigen-specific $CD4^+$ T cells from different donors were analysed under autologous or HLA-matched conditions. Release of IFN-γ by EBV-stimulated $CD4^+$ T cells was consistently reduced when co-cultured with wt versus ΔmirALL EBV-infected B cells as targets, both in autologous and HLA-matched situations (Fig. 16B). Importantly, $CD4^+$ T cells were not activated by mismatched infected B cells in this assay, indicating that the observed activation of $CD4^+$ T cells was EBV-specific and HLA class II-restricted (Fig. 16B).

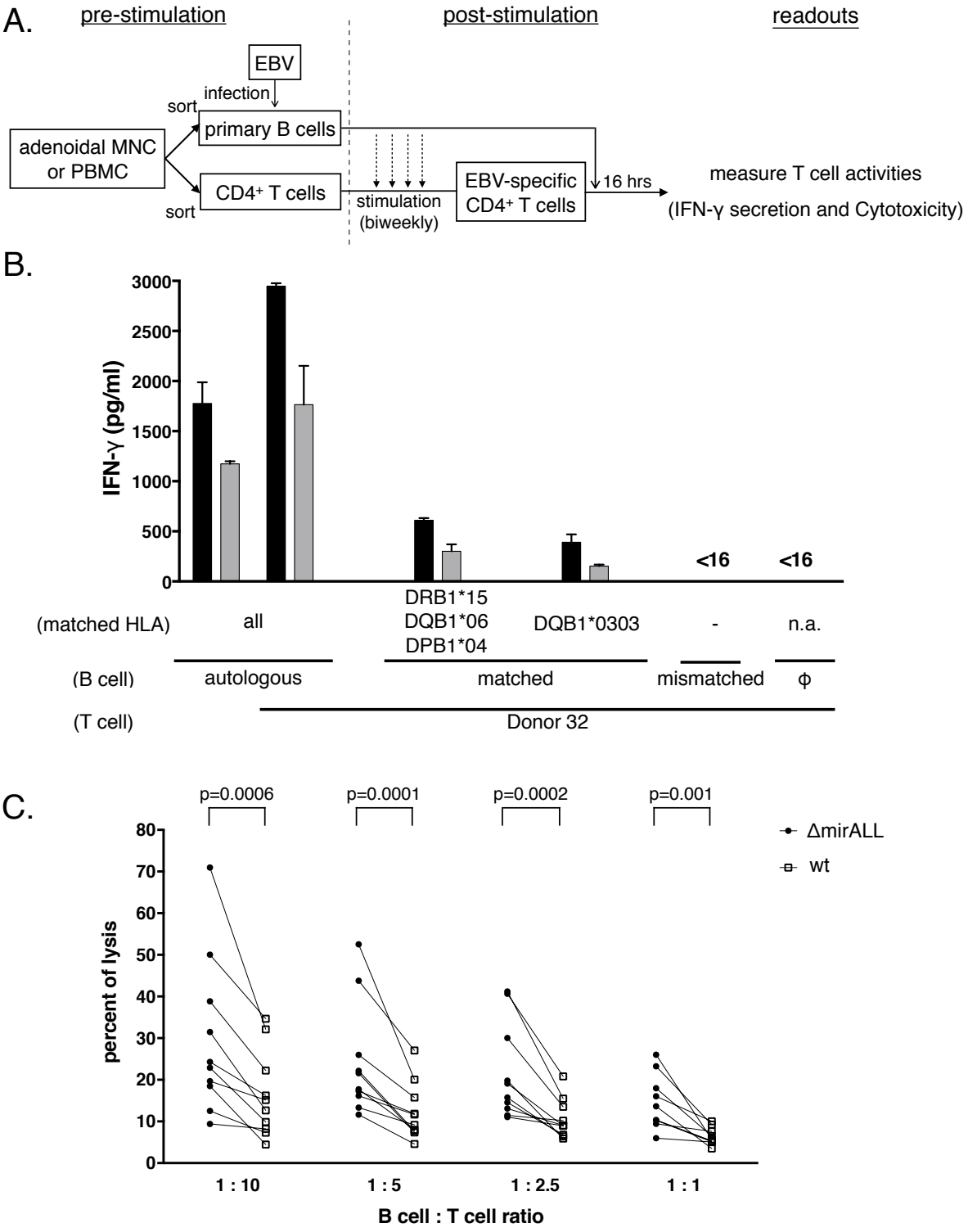

Figure 16 EBV miRNAs interfere with recognition and killing of infected B cells by CD4⁺ T cells
Recognition of EBV-infected B cells by EBV antigen-specific CD4⁺ T cells were assessed in co-culture experiments. In line with the reduced antigen presentation (Fig. 15), EBV antigen-specific CD4⁺ T cell secreted less IFN-γ and showed reduced cytotoxicity of EBV-infected B cells. It thus appeared that miRNAs encoded by wt EBV protect infected B cells from recognition by CD4⁺ T cells.

7.3 Protection of wt EBV-infected B cells from cytolytic effector CD4$^+$ T cells

EBV antigen-specific CD4$^+$ T cells have cytolytic activity (Adhikary et al., 2006). Thus, Albanese also tested this function in our co-culture assays. In allogeneic HLA-matched conditions, EBV antigen-specific CD4$^+$ T cells consistently showed stronger cytolysis of target B cells infected with ΔmirALL EBV than with wt EBV (Fig. 16C).

Taken together, EBV miRNAs negatively affected the recognition of infected B cells by HLA class II-restricted CD4$^+$ T cells, which showed an impaired cytokine secretion and reduced killing of the infected B cells early after infection.

(A) Schematic presentation of the co-culture experiment with EBV-stimulated T cells and B cells infected with wt or ΔmirALL EBV. CD4$^+$ T cell were isolated from PBMCs or adenoid biopsies, sorted, and stimulated with irradiated autologous EBV-infected B cells biweekly to expand CD4$^+$ EBV-specific effector T cells. Expanded CD4$^+$ T cells were cultivated with autologous, HLA-matched allogeneic, or mismatched B cells infected either with wt or with ΔmirALL EBV strains at day five post infection. IFN-γ secretion or cytotoxic effects on infected B cells were analyzed 16 hours later.

(B) Activation of EBV antigen-specific CD4$^+$ T cells with autologous, HLA-matched allogeneic, or mismatched B cells infected either with wt or with ΔmirALL EBV. The effector: target ratio was 1:1, the readout was IFN-γ secretion levels quantitated with ELISA. Both autologous and allogeneic CD4$^+$ T cells cultivated with wt EBV-infected cells secreted less IFN-γ compared with T cells cultivated with ΔmirALL EBV-infected cells, indicating that wt EBV-infected B cells are better protected from the recognition by effector CD4$^+$ T cells than ΔmirALL EBV-infected B cells. The HLA types of Donor 32 are as follows: HLA-DRB1*1501, HLA-DRB1*0701, HLA-DQB1*0602, HLA-DQB1*0303, HLA-DPB1*0401. Matched HLA types are shown. n.a: not applicable.

(C) Cytotoxic activities of EBV antigen-specific CD4$^+$ T cells. The cytotoxic capacity of CD4$^+$ T cells was analyzed with calcein release assays after co-culture with HLA-matched allogeneic B cells infected with wt or ΔmirALL EBV. The experiments were performed at various effector:target ratios as indicated. CD4$^+$ T cells killed more ΔmirALL EBV-infected B cells than wt EBV-infected B cells. wt EBV miRNAs thus protect EBV-infected B cells from cytotoxic EBV antigen-specific CD4$^+$ T cells. p-values of two-tailed ratio T test are shown.

Discussion

Primary B cells newly infected with EBV are a successful model to reveal the phenotypes and molecular mechanisms controlled by viral miRNAs

EBV miRNAs regulate apoptosis and the cell cycle five days post infection

EBV miRNAs have anti-apoptotic and pro-proliferative cellular functions early after infection (Feederle et al., 2011a; 2011b; Seto et al., 2010). In my transcriptome and KEGG enrichment analyses I confirmed that genes associated with apoptosis, the cell cycle, and p53 signaling were regulated by both wt EBV miRNAs and +mirBART EBV-unique miRNAs (Fig. 8, Fig. 9). These results are in line with previous observations of my group. Viral miRNAs promote the proliferation of newly infected B cells comparing B cells infected with wt and ΔmirALL EBV (Seto et al., 2010), or +mirBART and wt EBV (Vereide et al., 2013). The identified pathways included several pro-apoptotic genes such as *PMAIP1* (*NOXA*), *BAX*, and *BBC3* (PUMA). *PUMA* was published recently to be regulated by a viral miRNA, miR-BART5 (Choy et al., 2008). I also identified that *PMAIP1* as a novel direct target of ebv-miR-BART2.

The most important miRNAs with pro-proliferative functions are miRNAs of the BHRF1 cluster (Seto et al., 2010), but genes targeted by these miRNAs and responsible for the observed phenotypes are unknown (Grundhoff and Sullivan, 2011). In my experiment, I also did not identify genes that are directly regulated by BHRF1 miRNAs and contribute to anti-apoptotic or cell cycle progressive functions, but such genes may be contained within the top class of genes classified to be consistently down-regulated by viral miRNAs (Result section 2.2; Fig. 7). Taken together, my infection model with primary B cells in combination with transcriptome analysis has the potential to study the molecular mechanisms that underlie the cellular phenotypes.

The overlap between published targets of EBV miRNAs and down-regulated genes in my transcriptome analysis is limited

The de facto standard to depict the repressive abilities of EBV miRNAs is *IPO7* (Dölken et al., 2010; Klinke et al., 2014; Kuzembayeva et al., 2012; Skalsky et al., 2012; Vereide et al., 2013). Both my transcriptome analysis and AGO2 RIP-Seq are consistent with the previous findings that *IPO7* is a direct target of a single viral miRNA, miR-BART3, encoded

by both wt and +mirBART EBV (Fig. 2, Fig. 8B, Fig. 11). In my experiments, *IPO7* was among the top down-regulated genes comparing “wt vs. ΔmirALL”, and “+mirBART vs. ΔmirALL” EBV-infected B cells (Fig. 7B, Fig. 8B) supporting the view that the 136 genes in the intersection of the two data sets are canonical targets of miRNAs encoded by wt EBV (Result section 2.2; Fig. 7B).

Published target genes like *IPO7* (Dölken et al., 2010), *LY75* (Skalsky et al., 2012), or *BBC3* (Choy et al., 2008) were down-regulated by EBV miRNAs (Fig. 8B) in my model, but not every reported target behaved as expected in my experiments with B cells infected with different EBV strains. According to my transcriptome analysis, only a limited number of known targets were down-regulated. Reported EBV miRNA-targeted transcripts such as *MICB* (Nachmani et al., 2009), *DICER1* (Iizasa et al., 2010), *TOMM22* (Dölken et al., 2010), *CASP3* (Vereide et al., 2013), *DAZAP2* (Skalsky et al., 2012), or *NLRP3* (Haneklaus et al., 2012) showed no differences at transcript levels comparing wt versus ΔmirALL EBV-infected B cells (Fig. 8B, Supplementary Table 1). Among them, *TOMM22*, (Dölken et al., 2010) and *DAZAP2* (Skalsky et al., 2012) were even reported along with *IPO7* (*ibid.*) and *LY75* (*ibid.*), respectively, both of which were included in the top class of down-regulated genes mediated by viral miRNAs in my experiments (Fig. 6B). These discrepancies between my transcriptome analysis and previously reported targets may be due to two reasons.

First, the reported targets have been identified in established cell lines that differ from the primary infection model with newly infected primary B cells I employed. Cell lines in previous reports were of various origins and have been cultivated long-term in different conditions. These cell lines thus may have accumulated profound changes in their gene expression profiles. Using newly infected human primary B cells, a model that is close to primary infection *in vivo*, I could identify physiologically and virologically important targets of EBV miRNAs.

Second, translational repression induced by miRNAs occurs prior to the degradation of transcripts (Djuranovic et al., 2012). Because of this, not all miRNA-regulated genes can be detected by RNA-Seq (Guo et al., 2010). An alternative approach to identify miRNA-regulated genes is Ribosome-profiling. In most cases, differences in the level of transcripts obtained by Ribosome-profiling and RNA-Seq correlate, but Ribosome-profiling better reflects the effect of viral miRNAs on translational regulation as Ribosome-profiling record only actively translated mRNAs (Guo et al., 2010).

Immune regulatory pathways constitute canonical targets of viral miRNAs

In my transcriptome and KEGG enrichment analyses I found that not only pro-proliferative functions but also many immune regulatory pathways were regulated by viral miRNAs (Fig. 8A). This finding was particularly surprising because affected immune regulatory pathways ranged from innate immunity (TLR signaling, RIG-I-like receptor signaling, and Natural Killer cell mediated pathways) to adaptive immunity (antigen presentation, cytokine signaling, and cell adhesion molecules, which also encompass antigen presentation) suggesting that EBV miRNAs globally control immune responses in newly infected primary human B cells (Fig. 8A).

In fact, I observed that viral miRNAs reduced the secretion of IL-12 and IL-23, which promote helper T cell differentiation. Specifically the reduced IL-12 secretion abrogated the differentiation of naive $CD4^+$ T cells to type 1 helper T (Th1) cells, which have antiviral functions (Fig. 13, Fig. 14). Secretion of IL-6 and TNF-α was also controlled by EBV miRNAs but required TLR9 stimulation with CpG DNA for reliable detection (Fig. 13). These results suggest an important role of EBV miRNAs in mitigating the pro-inflammatory microenvironment that EBV infection may cause.

Moreover, we observed weaker antigen presentation by MHC class II molecules (Fig. 15) and reduced recognition of B cells infected with wt EBV compared with ΔmirALL EBV by effector $CD4^+$ T cells (Fig. 16). Similar to MHC class II molecules, MHC class I molecules were reduced in the early days of infection (Fig. 15) suggesting that EBV miRNAs inhibit antigen presentation of EBV-infected B cells to $CD8^+$ as well as to $CD4^+$ T cells.

Evasion from EBV antigen-specific $CD4^+$ T cell responses is thought to be particularly important early after infection. These $CD4^+$ T cells predominantly target viral structural antigens that are directly derived from virus particles and presented by MHC class II of EBV-infected cells immediately after infection (Adhikary et al., 2007). On the other hand, EBV antigen-specific $CD8^+$ T cells play their most important roles during the latent phase, because they mainly recognize epitopes from latent genes, complementing $CD4^+$ T cell activities directed against EBV during the other phases of EBV's life cycle (Mautner and Bornkamm, 2012). Our results indicated that all three signals, which are required for efficient recognition by effector T cells, i.e. antigen presentation (the first signal), co-stimulatory molecules (the second signal), and pro-inflammatory cytokines (the third signal)

are simultaneously down-regulated during the pre-latent phase (Kalla and Hammerschmidt, 2012) and in the early days of latent infection (Fig. 13, Fig. 14, Fig. 15, Fig. 16).

Everything considered, these findings indicate that EBV miRNAs govern many T cell immune responses covering all aspects from differentiation to antigen presentation and recognition throughout the entire EBV infection process.

Viral miRNAs encoded only by +mirBART EBV may regulate Fc receptors

In addition to cell proliferation and immune regulation, which are prominently highlighted in the KEGG enrichment analysis comparing “wt vs. ΔmirALL” EBV-infected B cells (Fig. 7B), Fc receptors may be among the specific targets of +mirBART EBV-unique miRNAs (Fig. 9). Many genes encoding Fc receptors that are classified as inhibitory BCR co-receptors such as *FCGR2B*, *FCRL2*, *FCRL4*, *FCRL5*, and *CD72* (Tsubata, 2012) were down-regulated at transcript levels in +mirBART compared with wt EBV-infected B cells (Fig. 9B). The only exception is the *FCRL1* gene, which is known to encode an activating BCR co-receptor (Leu et al., 2005). The transcripts of these genes were not down-regulated in wt compared with ΔmirALL EBV-infected B cells (Fig. 7B) suggesting that these genes are exclusively controlled by +mirBART EBV-unique miRNAs.

The natural ligands of most FCRLs are unknown, but the Fc portion of the IgG molecule is the ligand of FCGR2B (FcγRIIB; Tsubata, 2012). The receptor FCGR2B is activated by the antigen-Ig complex, which results in the apoptosis of mature naive B cells and plasma cells *in vitro* (Tzeng et al., 2005; Xiang et al., 2007). FCGR2B was expressed on the surface of EBV-infected B cells and was down-regulated by +mirBART EBV-unique miRNAs at day five post infection (Fig. 8B, Fig. 10D), which may prevent FCGR2B-induced apoptosis. The signaling pathways of other FCRLs, for which no ligands are known, are thought to inhibit BCR signaling (Tsubata, 2012). Therefore, it is possible that by controlling FCGR2B and FCRLs, +mirBART EBV-unique miRNAs protect EBV-infected B cells from apoptosis mediated by the activation of Fc receptors, which can be induced by various antibody-antigen complexes *in vivo*.

Indirect gene regulation by EBV miRNAs

EBV miRNAs have the potential to indirectly regulate a wide range of genes

In my transcriptome analysis, I found, along with consistently down-regulated genes, similar numbers of genes up-regulated by viral miRNAs (Fig. 7A). Since the main function of miRNAs is to down-regulate gene expression (Bartel, 2004), this result is counter-intuitive. It may be because viral miRNAs down-regulate genes like transcriptional repressors thereby indirectly up-regulate many genes without directly binding and regulating them.

Such indirectly regulated genes can be also seen in my comparative transcriptome analysis (Fig. 7B). Genes included in the intersections of the pair-wise comparisons of the data sets “wt vs. ΔmirALL”, “+mirBART vs. wt”, and “+mirBART vs. ΔmirALL” EBV-infected B cells are likely to be directly regulated targets of EBV miRNAs (Result section 2; Fig. 7B). However, the number of genes contained in the intersections is relatively small compared with all genes that were identified to belong to the top class of genese consistently down-regulated by viral miRNAs. For example, only 136 out of 748 genes in the “wt vs. ΔmirALL” comparison are included in the “+mirBART vs. ΔmirALL” comparison (Fig. 7B). Compared with ΔmirALL EBV-infected B cells, the remaining 612 genes appear to be down-regulated in wt but not in +mirBART EBV-infected B cells. Again, this result is counter-intuitive because +mirBART EBV includes all 13 miRNAs encoded by wt EBV, and thus the transcripts down-regulated by wt EBV should also be down-regulated in +mirBART EBV-infected B cells. A possible explanation for this observation is that +mirBART EBV-unique miRNAs indirectly up-regulate the 612 genes neutralizing or even reversing the repressive effects of the wt EBV miRNAs (see Fig. 17 with *MIR155HG* gene as an example).

Viral miRNAs regulate certain cell surface molecules beyond translational control

Inconsistencies between transcript and protein levels are an additional sign of indirect regulation by viral miRNAs. Genes like *CD86* and *CD274* were down-regulated at transcript levels in wt compared with ΔmirALL EBV-infected B, but the protein levels of both surface molecules did not correlated (Fig. 8B, Fig. 10C). These results may stem from the fact that viral miRNAs selectively hamper certain proteolytic pathways in EBV-infected cells leading to unaltered, or even elevated steady state levels of certain cellular proteins, independent of their reduced steady state transcript levels.

The indirect regulation of LMP1 by EBV miRNAs may be partly responsible for the unexpected regulation of cellular transcripts

The viral gene *BNLF1* (*LMP1*) is down-regulated in "wt vs. ΔmirALL" EBV-infected B cells, but is up-regulated in "+mirBART vs. wt" EBV-infected B cells (Fig. 17). LMP1 is known to up-regulate the expression of *MIR155HG* (*BIC*), which results in the up-regulation of miR-155, a miRNA hosted by the *BIC* transcript (Lu et al., 2008). In line with this report, *LMP1*, *BIC*, and miR-155 appeared to be regulated by viral miRNAs in my transcriptome analysis (Fig. 5B, Fig. 17). *LMP1* is reported to be directly controlled by multiple BART cluster miRNAs (miR-BART1, -BART16, and -BART17; Lo et al., 2007). Therefore, it is possible that EBV miRNAs directly down-regulate *LMP1*, which then leads to reduced *BIC* transcript levels and lower concentration of miR-155 in wt vs. ΔmirALL EBV-infected B cells (Fig. 5B, Fig. 17). As miR-155 is reported to negatively regulate a number of downstream genes (Elton et al., 2013), it is conceivable that the down-regulation of miR-155 by viral miRNAs results in the up-regulation of direct targets of miR-155. In fact, I found six out of 131 genes, which have been reported to be directly down-regulated by miR-155 (TarBase v7.0; Vlachos et al., 2015) and are counter-regulated with regard to *BIC*, *LMP1*, and miR-155 (Fig. 17).

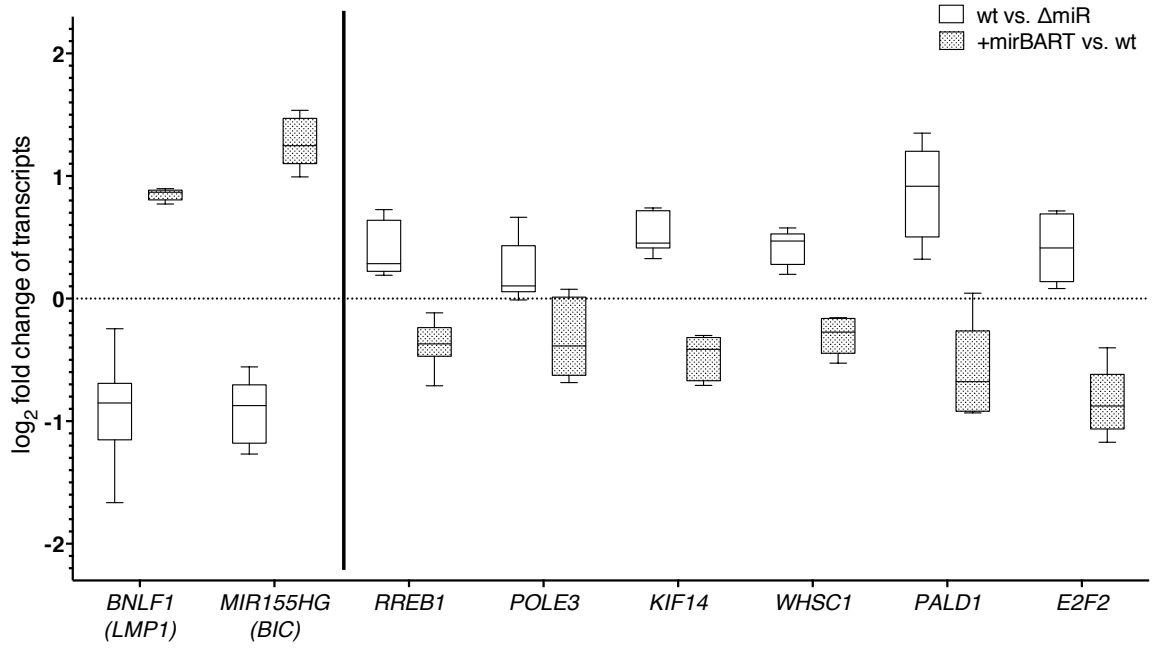

Figure 17 EBV miRNAs may indirectly regulate direct targets of miR-155 via LMP1

Box plots illustrating log2 fold changes of selected genes. *LMP1* and *BIC* (host gene of miR-155) transcript levels are strongly regulated by wt EBV miRNAs and +mirBART EBV-unique miRNAs. Six genes, which are previously reported to be targets of miR-155, are counter-regulated with respect to *LMP1* or *BIC*. EBV miRNAs may control *LMP1* which repress *BIC* and miR-155 expression hence leads to increased transcript levels of direct targets of miR-155.

To make matters even more complicated, my transcriptome analysis suggested that the control of *LMP1* by viral miRNAs is also partly indirect. This is because +mirBART EBV-infected B cells have higher LMP1 transcript level than wt EBV-infected B cells (Fig. 17) despite the fact that miR-BART16 and 17, which reportedly directly control *LMP1*, are encoded only by +mirBART EBV but not by wt EBV.

Taken together, EBV miRNAs control the expression of many cellular and certain viral genes directly and/or indirectly. As a result, they act not only as repressors but also as activators depending on the cellular context and regulatory factors, which control expression of other genes.

The identification of direct targets of viral miRNAs by AGO2 RIP-Seq

Enrichment scores revealed the direct binding of viral miRNAs to the 3'-UTR of *IPO7*

To identify transcripts directly bound by viral miRNAs, I compared the enrichment of AGO2 RIP-Seq reads in wt versus ΔmirALL EBV-infected B cells. For a quantitative evaluation, we introduced an enrichment score, which took into account the amount of RISC-trapped reads in wt compared with ΔmirALL EBV-infected cells at the level of the individual donors of B cells. *IPO7* is the most widely accepted target of viral miRNAs identified in the majority of high-throughput screens looking for direct targets of EBV miRNAs (Erhard et al., 2013; Klinke et al., 2014; Kuzembayeva et al., 2012; Riley et al., 2012; Skalsky et al., 2012; Vereide et al., 2013). In line with the publications, the transcript level of *IPO7* was also consistently down-regulated by wt EBV miRNA in my transcriptome analysis of all six donors (Fig. 8B). Since my AGO2 RIP-Seq data also had a high enrichment score at the exact binding site of miR-BART3, a reported EBV miRNA to control *IPO7* (Fig. 11), I concluded that, based on enrichment scores, my AGO2 RIP-Seq can principally capture mRNAs directly bound by viral miRNAs.

Viral miRNAs-regulated transcripts except *IPO7* are poorly enriched in wt EBV-infected B cells

Whereas enrichment scores of my AGO2 RIP-Seq data confirmed *IPO7* as a *bona fide* target (Fig. 11), top consistently down-regulated genes like *IL12B* or *PMAIP1* showed relatively poor enrichment scores on their transcripts (Result section 4.2; Fig. 11 bottom). The discrepancies between low RIP-Seq enrichment and high repression levels can be due to a differential degradation of mRNA molecules induced by viral miRNAs. It is possible that the degradation of viral miRNA-targeted transcripts in wt EBV-infected B cells was so strong that AGO2 RIP could not capture more reads of certain transcripts in wt compared with ΔmirALL EBV-infected B cells.

A possible solution is to employ a method similar to AGO2 RIP-Seq that is less dependent on relative transcript levels. Such methods are available and described as high-throughput sequencing of RNA isolated by crosslinking immunoprecipitation (HITS-CLIP; Chi et al., 2009) or individual-nucleotide resolution UV cross-linking and immunoprecipitation (iCLIP; König et al., 2010). These methods employ cross-linking of RISC and bound mRNAs using chemicals or UV such that the exact binding sites of miRNAs can be documented. It is still possible that extremely low expressed transcripts cannot be captured even by these technique, but comparing B cells infected with different EBV strains with these methods will provide binding sites that are present only in wt or +mirBART EBV-infected cells but not in ΔmirALL EBV-infected cells, which lack any viral miRNA. In short, utilizing cross-linking based screening approaches should increase the efficiency to identify direct targets of EBV miRNAs.

EBV miRNAs can robustly and cooperatively regulate targets

Multiple viral miRNAs redundantly control expression of important genes

To predict the direct targets of EBV miRNAs, I combined the enrichment scores calculated from my AGO2 RIP-Seq analysis, the transcriptome data, and 3'-UTR reporter assays. As a result, I identified *IL12B*, *PMAIP1*, *FCGR2B*, and *TGFBR2* as direct targets of EBV miRNAs (Fig. 7, Fig. 10, Fig. 11, Fig. 12).

The reporter with *IL12B* 3'-UTR was repressed by five miRNAs, which can target at least six binding sites in total (Fig. 12A, Supplementary Fig. 4). It thus appears that EBV miRNAs can redundantly repress certain target mRNAs like *IL12B.* This novel finding is surprising

but indicates a viral strategy directed against single-nucleotide polymorphisms (SNPs) within miRNA binding sites in 3'-UTRs, which may abrogate the down-regulation by miRNAs (Landi et al., 2008). Strangely, although *IL12B* is regulated by both wt EBV miRNAs and +mirBART EBV-unique miRNAs as discussed (Fig. 12A), *IL12B* did not fall into the intersection comparing "wt vs. ΔmirALL" and "+mirBART vs. wt" EBV-infected B cells according to my transcriptome analysis (Fig. 7B). In fact, only one gene was identified in this intersection (Fig. 7B). These observations imply that wt EBV miRNAs already suppress their direct targets so strongly that +mirBART EBV-unique miRNAs cannot additionally down-regulate transcripts like *IL12B*, which is possibly a sign of redundancy.

Interestingly, miRNAs that target *IL12B* stem from all three miRNA-encoding regions: the BHRF1 cluster (miR-BHRF1-2), the BART cluster (miR-BART1, miR-BART10, and miR-BART22), and the miR-BART2 coding region (Fig. 2, Figure 12), each of which are expressed from different promoters (Barth et al., 2011). This finding suggests that, even though the expressed miRNA may differ depending on cell types or the phase of infection (Cai et al., 2006; Qiu et al., 2011), *IL12B* will be down-regulated by miRNAs encoded by any of these clusters.

Moreover, I observed the down-regulation of *IL12B* (coding for IL-12p40) and *IL23A* (coding for p19) at transcript levels and the reduced secretion of the heterodimeric IL-23 cytokine (IL-12p40/p19) from EBV-infected B cells (Fig. 8B, Fig. 10, Fig. 13).

As discussed in this section, EBV miRNAs control important targets like *IL12B* redundantly at multiple levels: (i) many viral miRNAs simultaneously control the same transcripts using different binding sites; (ii) viral miRNAs targeting identical mRNAs are encoded on different primary EBV transcripts; (iii) transcripts, whose protein products form multimers are down-regulated concurrently.

EBV miRNAs cooperatively down-regulate *LTB*

LTB is the only gene included in the intersection of the comparison "wt vs. ΔmirALL" and "+mirBART vs. wt" EBV-infected B cells (Fig. 7B) indicating that LTB is down-regulated by wt EBV miRNAs and further down-regulated by +mirBART EBV-unique miRNAs. This finding implies a cooperative regulation by a multitude of viral miRNAs. The *in silico* prediction with TargetScan provided two possible binding sites located on the 3'-UTR of *LTB*. Only two wt EBV miRNAs (miR-BART2 and miR-BART3) were predicted suggesting

that +mirBART EBV-unique miRNAs regulate *LTB* indirectly. LTB or lymphotoxin-β is a cell surface molecule, which forms a complex with lymphotoxin-α. This complex is recognized by lymphotoxin-βreceptor (LTβR) expressed on follicular dendritic cells or dendritic cells (Upadhyay and Fu, 2013), enhancing both innate and adaptive immune responses. EBV-infected B cells will benefit from a robust and cooperative control of *LTB* by EBV miRNAs further supporting immune evasion of infected cells.

Taken together, viral miRNAs robustly and cooperatively regulate expression of certain important genes like *IL12B*, which support the survival of EBV-infected B cell *in vivo* in the immune-competent human host.

Conclusive Remarks

Among the genes encoded by EBV viral miRNAs have unique features. They constitute a highly clustered and large repertoire, which is unique and not conserved among miRNAs encoded by its host or other herpes viruses. It is thus conceivable that EBV miRNAs provide a wide range of functions unique to this virus. Typically, the main functions of miRNAs are dedicated to fine-tune gene expression, but the BHRF1 cluster miRNAs have dramatic effects on the proliferation and survival of EBV-infected B cells in the early days of infection.

Here, in this work, I extend these previous findings and discovered that EBV miRNAs have an enormous impact and control adaptive immune responses of the infected human host. Secretion of cytokines like IL-12 was reduced by viral miRNAs and this hampered the differentiation of antiviral type 1 helper T cells from naive $CD4^+$ T cells. EBV miRNAs also inhibited antigen presentation of EBV-infected cells protecting them from recognition and killing by EBV antigen-specific $CD4^+$ T cells. My work documented that EBV miRNAs have evolved to disrupt the adaptive immunity in the pre-latent phase of viral infection.

Materials & Methods

Nomenclature

EBV strain

I called the three EBV strains (ΔmirALL, wt/B95.8 or wt, +mirBART) used in this dissertation as in Seto et al., 2010 for the consistency to the previous work of the group.

Gene, transcripts, gene products, miRNA

For calling human genes, transcripts, and gene products, I followed the guideline of the HUGO Gene Nomenclature Committee. I applied the same rule for EBV genes. For miRNAs, I followed the nomenclature used in the miRBase (Kozomara et al., 2011, www.mirbase.org).

Cell culture, EBV production, and B cell infection

Separation of human primary cells

Human primary B and T cells were prepared from adenoidal mononuclear cells (MNC) or peripheral blood mononuclear cells (PBMC) by Ficoll-Hypaque gradient centrifugation. B cells, $CD4^+$ T cells, and naive $CD4^+$ T cells were separated from adenoidal MNC or PBMC using the MACS separator (Miltenyi Biotec) with the CD19 MicroBeads, the CD4 MicroBeads, and the Naive $CD4^+$ T cell Isolation Kit II, respectively (Miltenyi Biotec).

Cell lines and cell culture

The EBV-positive Burkitt's lymphoma cell line Raji and HEK293-based EBV producer cell lines (Seto et al., 2010), infected human primary B cells, and isolated T cells were maintained in RPMI 1640 medium (Life Technologies). HEK293T cells were maintained in DMEM medium. All media were supplemented with 10% FBS (Life Technologies), penicillin (100U/ml; Life Technologies), and streptomycin (100mg/ml; Life Technologies). Cells were cultivated at 37°C in a 5% CO_2 incubator.

Preparation of infectious EBV stocks and infection of human primary B cells

Infectious EBV stocks were prepared as described (Seto et al., 2010). Briefly, EBV producer cell lines for ΔmirALL and B95.8/wt (wt), and +mirBART EBV strain were transiently transfected with expression plasmids encoding *BZLF1* and *BALF4* to induce EBV's lytic cycle. I collected supernatants three days after transfection. Debrie was cleared by centrifugation at 3000rpm for 15 minutes. Virus stocks were titered on Raji cells as previously reported (Seto et al., 2010). For virus infection at a multiplicity of infection of 0.1 green Raji unit per ml, primary B cells were cultivated with each virus stock for 18hours. After replacement with fresh medium, the infected cells were seeded at an initial density of 5×10^5 cells per ml.

RNA-Seq

cDNA library preparation for RNA-Seq

From newly infected human primary B cells of six different donors (Ad1 to Ad6), I extracted total RNAs at day five post infection with Trizol (Life Technologies) and Direct-Zol RNA MiniPrep (Zymo Research) according to the manufacturers' protocols. The cDNA libraries were prepared by vertis Biotechnologie AG, Freising, Germany. Total RNAs were depleted of rRNAs by Ribo-Zero rRNA Removal Kit (illumina), fragmented by ultrasonication, and subjected to the first strand synthesis with a randomized primer. The cDNAs were PCR-amplified and sequenced (paired-end, 50 nucleotides from both sides) with an Illumina HiSeq2000 instrument at the University of Wisconsin Biotechnology Center DNA Sequencing Facility.

Sequencing, mapping, and data normalization

Processing of paired-end reads (poly-A tail filtering, N-filtering, adapter removal) was done using FastQC and R2M (RawReadManipulator). Reads were mapped to the human genome (hg19 'core' chromosome-set) by STAR (Dobin et al., 2012) and feature counts per transcript were determined using featureCounts (Liao et al., 2014) and GencodeCV19 annotations together with EBV's annotation (GenBank: AJ507799). Read Counts were normalized using DESeq2.

Fold change-based rank score and selecting differentially expressed genes

Since individual differences in gene expression seem to have a stronger impact than transcriptome alteration induced by EBV infection (see Fig. 5A) we used a simple but efficient

scoring algorithm based on donor-wise fold-change based ranks. For each transcript *t* and donor *k* we calculate the transcript-specific rank score $r_t = \frac{1}{m}\sum_{k=1}^{n} r_{tk}$ where *n* is the number of all donors, *m* the number of all transcripts, r_{gk} the rank of gene *g* in sample *k*. To select highly differentially expressed genes we transformed the rank score into a Z score, and all transcripts with an absolute Z score >1.6 were selected.

KEGG pathway enrichment analysis and PCA analysis

Enrichment of specific pathways was estimated by performing a hypergeometric distribution test via the KEGG API Web Service. Both KEGG pathway enrichment analysis and PCA analysis were done using Matlab (Mathworks).

AGO2 RIP-Seq

AGO2 RIP, deep sequencing, and mapping

1x10^8 EBV-infected B cells were lysed with 1ml lysis Buffer (20mM Tris (pH7.5), 150mM NaCl, 0.25% NP-40, 1.5mM $MgCl_2$, 1mM DTT, 40U/ml RNAsin (Promega), EDTA-free Complete tablet; Roche). The supernatant of lysed sample was incubated for four hours at 4°C with 60µl (3 mg of 11A9) anti-AGO2 antibody provided by Elizabeth Kremmer (Rüdel et al., 2008), which have been conjugated to MyOne Tosylactivated Dynabeads (Life Technologies). Dynabeads were washed three times (150mM Tris-HCl (pH7.0), 100mM Tris-HCl (pH8), 750 mM NaCl, 0.25% NP-40, 5mM $MgCl_2$, 1mM DTT), and co-precipitated RNA was extracted with Direct-Zol RNA MiniPrep (Zymo Research). In parallel, western blot analysis of the Dynabeads-bound AGO2 protein was performed after the last wash. Extracted RNAs were poly (A)-tailed, ligated to an RNA adapter at the 5'-phosphate group to facilitate Illumina TruSeq sequencing, and subjected to first strand synthesis with a oligo-(dT) primer. Subsequent PCR amplification, deep sequencing (single-ended, 50 nucleotides), and mapping were performed as described in the RNA-Seq section above.

Calculating the enrichment score

Mapped reads from AGO2 RIP-Seqs were normalized to the total number of reads in the samples of each donor. To quantitate the enrichment of reads at each position of the 3'-UTRs of interest in wt EBV compared with ΔmirALL EBV-infected B cells, we defined an enrichment score. First, we calculated a parameter $e_{up} = \frac{t_{up}}{t_{up}+c_{up}} \cdot \frac{t_{up}}{\max(t_u)}$, where *u* is the 3'-UTR of

interest, p is the position within u, t and c is the normalized numbers of mapped reads in wt and ΔmirALL EBV-infected B cell, respectively. The max(t_u) is the maximum number within t_u. The e_{up} was calculated for each donor and modified using Gaussian smoothing (gauss2d.m in Matlab). To select 3'-UTRs bound by viral miRNAs, we set the threshold as follows: enrichment score >0.6 for a stretch of >20 nucleotides in the 3'-UTRs in two or more donors.

Quantification of protein levels

ELISA

To detect cytokine secretion from infected B cells, $1x10^6$ cells were seeded in 6 well plates at four or eleven days post infection and cultivated for four additional days with cyclosporine (1µg/ml; Novartis). Supernatants were collected and stored at -20°C. Enzyme-linked immunosorbent assays (ELISAs) for interleukin-6 (IL-6), IL-10, IL12B (p40), IL-12, IL-23, and TNF-α were performed following the manufacturer's protocol (Mabtech). For IL-6, IL-10, and TNF-α, CpG DNA was added as previously described (Iskra et al., 2010) to induce the secretion of cytokines from EBV-infected B cells.

ELISAs to quantify IFN-γ levels in the co-culture experiments were performed following the manufacturer's protocol (Mabtech).

Western blot analysis

Cells were lysed with RIPA buffer (50mM Tris-HCl (pH 8), 150mM NaCl, 0.1% SDS, 1% NP-40, 0.5% DOC) and boiled with Laemmli buffer. Proteins were separated on 10% SDS-PAGE gels (Carl Roth) and transferred to nitrocellulose membranes (Amersham) using Mini-PROTEAN Tetra Cell (Bio-Rad). Membranes were blocked for 30 minutes with Roti-Block (Carl Roth) followed by antibody incubation. Protein levels were quantitated with the Odyssey CLx (LI-COR) Imager. The following primary antibodies directed against human proteins were used: anti-human Tubulin (B-5-1-2, Santa Cruz, 1:2500), anti-human Actin (AC-74, Sigma, 1:10000), anti-human PMAIP1 (FL-54, Santa Cruz, 1:200), and anti-human AGO2 (C34C6, Cell signaling, 1:500).

Flow cytometry of cell surface proteins

After immunostainings with fluorophore-conjugated antibodies, single-cell suspensions were measured with the aid of LSRFortessa or a FACSCanto (BD) flow cytometers equipped with the FACSDiva software (BD Biosciences). Acquired data were analysed with the FlowJo software Ver. 9.8 (FlowJo).

The following fluorophore-conjugated antibodies directed against human antigens were used: APC anti-human IFN-γ (4S.B3; BioLegend), anti-CD40 PE (5c3, IgG2b; BioLegend), anti-ICOS-L PE (2D3, IgG2b; BioLegend), anti-PD-L1 (CD274) APC (29E.2A3, IgG2b; BioLegend), anti-CD86 PE (37301, IgG1; R&D Systems), anti-CD32 (FCGR2B) PE (FUN-2, IgG2b; BioLegend), anti-FCRL4 PE (413D12, IgG2b; BioLegend), anti-HLA-ABC APC (W6/32, IgG2a; BioLegend), anti-Lambda PE (HP6054, IgG2a, ThermoFischer), anti-Kappa APC (HP6062, IgG3, ThermoFisher), anti-CD80 PE-Cy5 (L307.4; BD Pharmingen), anti-HLA-DR unlabeled (L234, IgG2a; BioLegend), anti-HLA-DQ unlabeled (SPV-L3, IgG2a ; AbD Serotec), anti-HLA-DP unlabeled (B7/21, IgG3; Abcam), anti-mouse F(ab')2 APC (Policlonal, IgG; eBioscience), isotype IgG1 PE (MOPC-21; BioLegend), isotype IgG2b PE (MPC-11; BioLegend), isotype IgG2a APC (MOPC-173; BioLegend), isotype IgG2b APC (MG2b-57; BioLegend), isotype IgG2a PE (MOPC-173; BioLegend), isotype IgG3 APC (MG305; Invitrogen).

Prediction and validation of miRNA targets

In silico prediction of miRNA binding sites

I performed *in silico* predictions of EBV miRNA binding sites on 3'-UTRs primarily with TargetScan6.2 (Garcia et al., 2011) and employed RNAhybrid (Rehmsmeier et al., 2004) to screen for 6mer binding sites (Bartel, 2009).

Luciferase reporter assay validation

The 3'-UTRs of *IL12B* (NM_002187), *PMAIP1* (NM_021127.2), FCGR2B (NM_004001), and *TGFBR2* (NM_003242) were cloned downstream of Firefly luciferase (*Fluc*) in the expression plasmid psiCHECK-2 (Promega). To construct the viral miRNA expression vectors, we cloned *TagBFP* (Evrogen) under the control of the EF1α promoter into pCDH-EF1-MCS (System Biosciences). Single miRNAs of interest were cloned downstream of the TagBFP-encoding

gene. Viral miRNAs were obtained by PCR from the p4080 plasmid (Seto et al., 2010). 50 ng of the psiCHECK-2 reporter and 150ng of pCDH-EF1 miRNA expresser plasmid DNAs were co-transfected into 1×10^5 HEK293T (seeded in 24-well plate on the previous day) with 0.9µl Metafectene Pro (Biontex). After 24 hours of transfection, the medium was discarded and 100µl Passive Lysis Buffer (Promega) followed by the incubation for 15 minutes while shaking (3D Sunflower shaker, bioSan). I measured luciferase activities with the aid of the Dual-Luciferase Assay Kit (50µl of Luciferase Assay Reagent II and Stop & Glow Buffer for each sample, Promega) and the Orion II Microplate Luminometer (Titertek-Berthold). The activity of Fluc was normalized by the activity of Renilla luciferase (Rluc) encoded in the psiCHECK-2 reporter. We performed site-directed mutagenesis with overlapping oligo DNAs and Phusion polymerase (New England Biolabs, Fig. 8E).

Co-culture experiments of naive CD4$^+$ T cells with EBV-infected B cells

Th1 differentiation was assessed in co-culture experiments of sorted human naive CD4$^+$ T cells with autologous B cells that have been infected with EBV and cultivated for five days. 1×10^5 naive CD4$^+$ T cells stained with CellTrace Violet (Life Technologies) and 0.5 or 1×10^5 infected B cells were co-cultured in 96 well plates with Dynabeads Human T-Activator CD3/CD28 (Life Technologies), and cultivated for 7 days following the manufacturer's instructions. The neutralizing antibody against IL12B (C8.6; BioLegend) or its isotype antibody (MOPC-21; BioLegend) was added for certain experiments (Fig. 10D) at 5µg/ml. Cells were re-stimulated with PMA and Ionomycin (Cell Stimulation Cocktail; eBioscience) for 5 hours and treated with Brefeldin A/Monensin (BioLegend) for 2.5hours prior to fixation. The Th1 population was determined via intracellular IFN-γ staining with the FIX & PERM Cell Permeabilization Kit (Life Technologies) and subsequent flow cytometry analysis. Since only CD3/CD28-stimulated T cells will proliferate, the Th1 population was defined as IFN-γ positive proliferating T cells. T cells with low CellTrace Violet staining were identified to be proliferating cells.

$CD4^+$ T cells stimulation experiments with EBV-infected B cells

Establishment of EBV antigen-specific effector T cells and T cell clones

Polyclonal EBV antigen-specific $CD4^+$ T cells were established from PBMCs by CD4 MACS and repetitive stimulations with lymphoblastoid cell lines (LCLs) as previously described (Adhikary et al., 2007).

IFN-γ release from T cells recognizing EBV-infected B cells

IFN-γ release from LCL-stimulated, EBV antigen-specific T cells (effector cells) co-cultured with EBV-infected B cells (target cells) was measured to assess the antigen presentation by infected B cells. Effector T cells and target B cells were seeded at $5x10^4$ cell per ml (1:1 ratio, unless otherwise mentioned) each and co-cultured for 16hours in a 96-well plate (V bottom). IFN-γ levels were detected with ELISA. IFN-γ concentrations lower than 16pg/ml were considered to be below the detection limit ("not detected").

Killing of EBV-infected B cells by T cells using the calcein release assay

Killing activity of EBV-infected B cells by EBV antigen-specific T cells was measured with the calcein release assay. EBV-infected B cells were purified by Ficoll-Hypaque gradient centrifugation and the $5x10^5$ target cells were labeled with calcein at 0.5µg/ml. After three washing steps with PBS, target and effector cells (EBV-stimulated T cells) were co-cultured in a 96-well plate (V bottom) with different ratios in RPMI red phenol-free medium to reduce background signals. After four hours of co-culture, fluorescence intensities of released calcein were measured with the aid of the Infinite F200 PRO fluorometer (Tecan). As controls, spontaneous calcein release of target cells cultivated without effector cells and completely lysed cells (0.5% Triton-X100) were used to define the levels of no and fully lysed target cells, respectively.

Statistical analysis

I used the Prism 6.0 software (GraphPad) for all my statistical analyses. The two-tailed ratio T test was applied unless otherwise mentioned.

Reference

Adhikary, D., Behrends, U., Boerschmann, H., Pfünder, A., Burdach, S., Moosmann, A., Witter, K., Bornkamm, G.W., and Mautner, J. (2007). Immunodominance of lytic cycle antigens in Epstein-Barr virus-specific CD4+ T cell preparations for therapy. PLoS ONE *2*, e583.

Adhikary, D., Behrends, U., Moosmann, A., Witter, K., Bornkamm, G.W., and Mautner, J. (2006). Control of Epstein-Barr virus infection in vitro by T helper cells specific for virion glycoproteins. J. Exp. Med. *203*, 995–1006.

Agarwal, V., Bell, G.W., Nam, J.-W., and Bartel, D.P. (2015). Predicting effective microRNA target sites in mammalian mRNAs. Elife *4*.

Bartel, D.P. (2004). MicroRNAs: genomics, biogenesis, mechanism, and function. Cell *116*, 281–297.

Bartel, D.P. (2009). MicroRNAs: target recognition and regulatory functions. Cell *136*, 215–233.

Barth, S., Meister, G., and Grässer, F.A. (2011). EBV-encoded miRNAs. Biochim. Biophys. Acta *1809*, 631–640.

Blum, J.S., Wearsch, P.A., and Cresswell, P. (2013). Pathways of antigen processing. Annu. Rev. Immunol. *31*, 443–473.

Cai, X., Schäfer, A., Lu, S., Bilello, J.P., Desrosiers, R.C., Edwards, R., Raab-Traub, N., and Cullen, B.R. (2006). Epstein–Barr Virus MicroRNAs Are Evolutionarily Conserved and Differentially Expressed. PLoS Pathog. *2*, e23.

Chi, S.W., Zang, J.B., Mele, A., and Darnell, R.B. (2009). Argonaute HITS-CLIP decodes microRNA-mRNA interaction maps. Nature *460*, 479–486.

Choy, E.Y.-W., Siu, K.-L., Kok, K.-H., Lung, R.W.-M., Tsang, C.M., To, K.F., Kwong, D.L.-W., Tsao, S.W., and Jin, D.-Y. (2008). An Epstein-Barr virus-encoded microRNA targets PUMA to promote host cell survival. J. Exp. Med. *205*, 2551–2560.

Cullen, B.R. (2013). MicroRNAs as mediators of viral evasion of the immune system. Nat. Immunol. *14*, 205–210.

Dahlke, C., Maul, K., Christalla, T., Walz, N., Schult, P., Stocking, C., and Grundhoff, A. (2012). A microRNA Encoded by Kaposi Sarcoma-Associated Herpesvirus Promotes B-Cell Expansion In Vivo. PLoS ONE *7*, e49435.

Delecluse, H.J., Pich, D., Hilsendegen, T., Baum, C., and Hammerschmidt, W. (1999). A first-generation packaging cell line for Epstein-Barr virus-derived vectors. Proc. Natl. Acad. Sci. U.S.A. *96*, 5188–5193.

Djuranovic, S., Nahvi, A., and Green, R. (2012). miRNA-Mediated Gene Silencing by Translational Repression Followed by mRNA Deadenylation and Decay. Science *336*, 237–240.

Dobin, A., Davis, C.A., Schlesinger, F., Drenkow, J., Zaleski, C., Jha, S., Batut, P., Chaisson, M., and Gingeras, T.R. (2012). STAR: ultrafast universal RNA-seq aligner. Bioinformatics *29*, bts635–21.

Dölken, L., Malterer, G., Erhard, F., Kothe, S., Friedel, C.C., Suffert, G., Marcinowski, L., Motsch, N., Barth, S., Beitzinger, M., et al. (2010). Systematic analysis of viral and cellular microRNA targets in cells latently infected with human gamma-herpesviruses by RISC immunoprecipitation assay. Cell Host Microbe *7*, 324–334.

Elton, T.S., Selemon, H., Elton, S.M., and Parinandi, N.L. (2013). Regulation of the MIR155 host gene in physiological and pathological processes. Gene *532*, 1–12.

Erhard, F., Dölken, L., Jaskiewicz, L., and Zimmer, R. (2013). PARma: identification of microRNA target sites in AGO-PAR-CLIP data. Genome Biol. *14*, R79.

Feederle, R., Haar, J., Bernhardt, K., Linnstaedt, S.D., Bannert, H., Lips, H., Cullen, B.R., and Delecluse, H.J. (2011a). The Members of an Epstein-Barr Virus MicroRNA Cluster Cooperate To Transform B Lymphocytes. J. Virol. *85*, 9801–9810.

Feederle, R., Linnstaedt, S.D., Bannert, H., Lips, H., Bencun, M., Cullen, B.R., and Delecluse, H.-J. (2011b). A viral microRNA cluster strongly potentiates the transforming properties of a human herpesvirus. PLoS Pathog. *7*, e1001294.

Filipowicz, W., Bhattacharyya, S.N., and Sonenberg, N. (2008). Mechanisms of post-transcriptional regulation by microRNAs: are the answers in sight? Nat. Rev. Genet. *2008*, 102–114.

Garcia, D.M., Baek, D., Shin, C., Bell, G.W., Grimson, A., and Bartel, D.P. (2011). Weak seed-pairing stability and high target-site abundance decrease the proficiency of lsy-6 and other microRNAs. Nat. Struct. Mol. Biol. *18*, 1139–1146.

Gottwein, E., Mukherjee, N., Sachse, C., Frenzel, C., Majoros, W.H., Chi, J.-T.A., Braich, R., Manoharan, M., Soutschek, J., Ohler, U., et al. (2007). A viral microRNA functions as an orthologue of cellular miR-155. Nature *450*, 1096–1099.

Grundhoff, A., and Sullivan, C.S. (2011). Virus-encoded microRNAs. Virology *411*, 325–343.

Guo, H., Ingolia, N.T., Weissman, J.S., and Bartel, D.P. (2010). Mammalian microRNAs predominantly act to decrease target mRNA levels. Nature *466*, 835–840.

Ha, M., and Kim, V.N. (2014). Regulation of microRNA biogenesis. Nat. Rev. Mol. Cell Biol. *15*, 509–524.

Haneklaus, M., Gerlic, M., Kurowska-Stolarska, M., Rainey, A.-A., Pich, D., McInnes, I.B., Hammerschmidt, W., O'Neill, L.A.J., and Masters, S.L. (2012). Cutting edge: miR-223 and EBV miR-BART15 regulate the NLRP3 inflammasome and IL-1β production. J. Immunol. *189*, 3795–3799.

Hislop, A.D., Annels, N.E., Gudgeon, N.H., Leese, A.M., and Rickinson, A.B. (2002). Epitope-specific evolution of human CD8(+) T cell responses from primary to persistent phases of Epstein-Barr virus infection. J. Exp. Med. *195*, 893–905.

Hislop, A.D., Ressing, M.E., van Leeuwen, D., Pudney, V.A., Horst, D., Koppers-Lalic, D., Croft, N.P., Neefjes, J.J., Rickinson, A.B., and Wiertz, E.J.H.J. (2007). A CD8+ T cell immune evasion protein specific to Epstein-Barr virus and its close relatives in Old World primates. J. Exp. Med. *204*, 1863–1873.

Iizasa, H., Wulff, B.E., Alla, N.R., Maragkakis, M., Megraw, M., Hatzigeorgiou, A., Iwakiri, D., Takada, K., Wiedmer, A., Showe, L., et al. (2010). Editing of Epstein-Barr Virus-encoded BART6 MicroRNAs Controls Their Dicer Targeting and Consequently Affects Viral Latency. J. Biol. Chem. *285*, 33358–33370.

Iskra, S., Kalla, M., Delecluse, H.J., Hammerschmidt, W., and Moosmann, A. (2010). Toll-Like Receptor Agonists Synergistically Increase Proliferation and Activation of B Cells by Epstein-Barr Virus. J. Virol. *84*, 3612–3623.

Jochum, S., Moosmann, A., Lang, S., Hammerschmidt, W., and Zeidler, R. (2012). The EBV Immunoevasins vIL-10 and BNLF2a Protect Newly Infected B Cells from Immune Recognition and Elimination. PLoS Pathog. *8*, e1002704.

Kalla, M., and Hammerschmidt, W. (2012). Human B cells on their route to latent infection – Early but transient expression of lytic genes of Epstein-Barr virus. European J. Cell Biol. *91*, 65–69.

Klinke, O., Feederle, R., and Delecluse, H.-J. (2014). Genetics of Epstein-Barr virus microRNAs. Semin. Cancer Biol. *26*, 52–59.

Kozomara, A., and Griffiths-Jones, S. (2011). miRBase: integrating microRNA annotation and deep-sequencing data. Nucleic Acids Res. *39*, D152–D157.

König, J., Zarnack, K., Rot, G., Curk, T., Kayikci, M., Zupan, B., Turner, D.J., Luscombe, N.M., and Ule, J. (2010). iCLIP reveals the function of hnRNP particles in splicing at individual nucleotide resolution. Nat. Struct. Mol. Biol. *17*, 909–915.

Kuzembayeva, M., Chiu, Y.-F., and Sugden, B. (2012). Comparing proteomics and RISC immunoprecipitations to identify targets of Epstein-Barr viral miRNAs. PLoS ONE *7*, e47409.

Landi, D., Gemignani, F., Barale, R., and Landi, S. (2008). A catalog of polymorphisms falling in microRNA-binding regions of cancer genes. DNA Cell Biol. *27*, 35–43.

Landthaler, M., Gaidatzis, D., Rothballer, A., Chen, P.Y., Soll, S.J., Dinic, L., Ojo, T., Hafner, M., Zavolan, M., and Tuschl, T. (2008). Molecular characterization of human Argonaute-containing ribonucleoprotein complexes and their bound target mRNAs. Rna *14*, 2580–2596.

Leu, C.-M., Davis, R.S., Gartland, L.A., Fine, W.D., and Cooper, M.D. (2005). FcRH1: an activation coreceptor on human B cells. Blood *105*, 1121–1126.

Liao, Y., Smyth, G.K., and Shi, W. (2014). featureCounts: an efficient general purpose program for assigning sequence reads to genomic features. Bioinformatics *30*, 923–930.

Liu, J., Rivas, F.V., Wohlschlegel, J., Yates, J.R., III, Parker, R., and Hannon, G.J. (2005a). A role for the P-body component, GW182, in microRNA function. Nat. Cell Biol. *7*, 1261–1266.

Liu, J., Valencia-Sanchez, M.A., Hannon, G.J., and Parker, R. (2005b). MicroRNA-dependent localization of targeted mRNAs to mammalian P-bodies. Nat. Cell Biol. *7*, 719–723.

Lo, A.K.F., To, K.F., Lo, K.W., Lung, R.W.-M., Hui, J.W.Y., Liao, G., and Hayward, S.D. (2007). Modulation of LMP1 protein expression by EBV-encoded microRNAs. Proc. Natl. Acad. Sci. U.S.A. *104*, 16164–16169.

Lu, F., Weidmer, A., Liu, C.-G., Volinia, S., Croce, C.M., and Lieberman, P.M. (2008). Epstein-Barr virus-induced miR-155 attenuates NF-kappaB signaling and stabilizes latent virus persistence. J. Virol. *82*, 10436–10443.

Mautner, J., and Bornkamm, G.W. (2012). The role of virus-specific CD4+ T cells in the control of Epstein-Barr virus infection. Eur. J. Cell Biol. *91*, 31–35.

Meister, G., Landthaler, M., Patkaniowska, A., Dorsett, Y., Teng, G., and Tuschl, T. (2004). Human Argonaute2 mediates RNA cleavage targeted by miRNAs and siRNAs. Mol. Cell *15*, 185–197.

Nachmani, D., Stern-Ginossar, N., Sarid, R., and Mandelboim, O. (2009). Diverse herpesvirus microRNAs target the stress-induced immune ligand MICB to escape recognition by natural killer cells. Cell Host Microbe *5*, 376–385.

Olive, V., Li, Q., and He, L. (2013). mir-17-92: a polycistronic oncomir with pleiotropic functions. Immunol. Rev. *253*, 158–166.

Pfeffer, S., Sewer, A., Lagos-Quintana, M., Sheridan, R., Sander, C., Grässer, F.A., van Dyk, L.F., Ho, C.K., Shuman, S., Chien, M., et al. (2005). Identification of microRNAs of the herpesvirus family. Nat. Meth. *2*, 269–276.

Qiu, J., Cosmopoulos, K., Pegtel, M., Hopmans, E., Murray, P., Middeldorp, J., Shapiro, M., and Thorley-Lawson, D.A. (2011). A novel persistence associated EBV miRNA expression profile is disrupted in neoplasia. PLoS Pathog. *7*, e1002193.

Rancan, C., Schirrmann, L., Hüls, C., Zeidler, R., and Moosmann, A. (2015). Latent Membrane Protein LMP2A Impairs Recognition of EBV-Infected Cells by CD8+ T Cells. PLoS Pathog. *11*, e1004906.

Rehmsmeier, M., Steffen, P., Hochsmann, M., and Giegerich, R. (2004). Fast and effective prediction of microRNA/target duplexes. Rna *10*, 1507–1517.

Ressing, M.E., Horst, D., Griffin, B.D., Tellam, J., Zuo, J., Khanna, R., Rowe, M., and Wiertz, E.J.H.J. (2008). Epstein-Barr virus evasion of CD8(+) and CD4(+) T cell immunity via concerted actions of multiple gene products. Semin. Cancer Biol. *18*, 397–408.

Riley, K.J., Rabinowitz, G.S., Yario, T.A., Luna, J.M., Darnell, R.B., and Steitz, J.A. (2012). EBV and human microRNAs co-target oncogenic and apoptotic viral and human genes during latency. Embo J. *31*, 2207–2221.

Rowe, M., Glaunsinger, B., van Leeuwen, D., Zuo, J., Sweetman, D., Ganem, D., Middeldorp, J., Wiertz, E.J.H.J., and Ressing, M.E. (2007). Host shutoff during productive Epstein-Barr virus infection is mediated by BGLF5 and may contribute to immune evasion. Proc. Natl. Acad. Sci. U.S.A. *104*, 3366–3371.

Rüdel, S., Flatley, A., Weinmann, L., Kremmer, E., and Meister, G. (2008). A multifunctional human Argonaute2-specific monoclonal antibody. Rna *14*, 1244–1253.

Schickel, R., Boyerinas, B., Park, S.-M., and Peter, M.E. (2008). MicroRNAs: key players in the immune system, differentiation, tumorigenesis and cell death. Oncogene *27*, 5959–5974.

Selbach, M., Schwanhäusser, B., Thierfelder, N., Fang, Z., Khanin, R., and Rajewsky, N. (2008). Widespread changes in protein synthesis induced by microRNAs. Nature *455*, 58–63.

Seto, E., Moosmann, A., Grömminger, S., Walz, N., Grundhoff, A., and Hammerschmidt, W. (2010). Micro RNAs of Epstein-Barr Virus Promote Cell Cycle Progression and Prevent Apoptosis of Primary Human B Cells. PLoS Pathog. *6*, e1001063.

Sevignani, C., Calin, G.A., Siracusa, L.D., and Croce, C.M. (2006). Mammalian microRNAs: a small world for fine-tuning gene expression. Mamm. Genome *17*, 189–202.

Skalsky, R.L., and Cullen, B.R. (2010). Viruses, microRNAs, and Host Interactions. Annu. Rev. Microbiol. *64*, 123–141.

Skalsky, R.L., Corcoran, D.L., Gottwein, E., Frank, C.L., Kang, D., Hafner, M., Nusbaum, J.D., Feederle, R., Delecluse, H.-J., Luftig, M.A., et al. (2012). The Viral and Cellular MicroRNA Targetome in Lymphoblastoid Cell Lines. PLoS Pathog. *8*, e1002484.

Stern-Ginossar, N., Elefant, N., Zimmermann, A., Wolf, D.G., Saleh, N., Biton, M., Horwitz, E., Prokocimer, Z., Prichard, M., Hahn, G., et al. (2007). Host immune system gene targeting by a viral miRNA. Science *317*, 376–381.

Strasser, A. (2005). The role of BH3-only proteins in the immune system. Nat. Rev. Immunol. *5*, 189–200.

Szabo, S.J., Sullivan, B.M., Peng, S.L., and Glimcher, L.H. (2003). Molecular mechanisms regulating Th1 immune responses. Annu. Rev. Immunol. *21*, 713–758.

Tsubata, T. (2012). Role of inhibitory BCR co-receptors in immunity. Infect. Disord. Drug Targets *12*, 181–190.

Tzeng, S.-J., Bolland, S., Inabe, K., Kurosaki, T., and Pierce, S.K. (2005). The B cell inhibitory Fc receptor triggers apoptosis by a novel c-Abl family kinase-dependent pathway. J. Biol. Chem. *280*, 35247–35254.

Upadhyay, V., and Fu, Y.-X. (2013). Lymphotoxin signalling in immune homeostasis and the control of microorganisms. Nat. Rev. Immunol. *13*, 270–279.

Vereide, D.T., Seto, E., Chiu, Y.-F., Hayes, M., Tagawa, T., Grundhoff, A., Hammerschmidt, W., and Sugden, B. (2014). Epstein-Barr virus maintains lymphomas via its miRNAs. Oncogene *33*, 1258–1264.

Vlachos, I.S., Paraskevopoulou, M.D., Karagkouni, D., Georgakilas, G., Vergoulis, T., Kanellos, I., Anastasopoulos, I.-L., Maniou, S., Karathanou, K., Kalfakakou, D., et al. (2015). DIANA-TarBase v7.0: indexing more than half a million experimentally supported miRNA:mRNA interactions. Nucleic. Acids. Res. *43*, D153–D159.

Walz, N., Christalla, T., Tessmer, U., and Grundhoff, A. (2009). A Global Analysis of Evolutionary Conservation among Known and Predicted Gammaherpesvirus MicroRNAs. J. Virol. *84*, 716–728.

Xia, T., O'Hara, A., Araujo, I., Barreto, J., Carvalho, E., Sapucaia, J.B., Ramos, J.C., Luz, E., Pedroso, C., Manrique, M., et al. (2008). EBV microRNAs in primary lymphomas and targeting of CXCL-11 by ebv-mir-BHRF1-3. Cancer Res. *68*, 1436–1442.

Xiang, Z., Cutler, A.J., Brownlie, R.J., Fairfax, K., Lawlor, K.E., Severinson, E., Walker, E.U., Manz, R.A., Tarlinton, D.M., and Smith, K.G.C. (2007). FcgammaRIIb controls bone marrow plasma cell persistence and apoptosis. Nat. Immunol. *8*, 419–429.

Xiao, C., and Rajewsky, K. (2009). MicroRNA control in the immune system: basic principles. Cell *136*, 26–36.

Zuo, J., Currin, A., Griffin, B.D., Shannon-Lowe, C., Thomas, W.A., Ressing, M.E., Wiertz, E.J.H.J., and Rowe, M. (2009). The Epstein-Barr virus G-protein-coupled receptor contributes to immune evasion by targeting MHC class I molecules for degradation. PLoS Pathog. *5*, e1000255.

Appendix

Contributions

Manuel Albanese (Research Unit Gene Vectors, Helmholtz Zentrum München) performed experiments and analysis described in the following figures:

Figure 7B, 7C, 12, 13

Jonathan Hoser and Maximilian Hastreiter (Institute of Bioinformatics and System Biology, Helmholtz Zentrum München) performed bioinformatical analyses that were the basis for the following figures:

Figure 1B, 1C, 2A, 2B

Dominik Lutter (Institute for Diabetes and Obesity, Helmholtz Zentrum München) performed bioinformatical analyses that was used in the following figures and data sets:

Figure 3, 4A, 5A, 6A, 8

Supplementary Figure 1, 2

Supplementary Table 1, 2

I performed all the experiments and analyses that are not mentioned above.

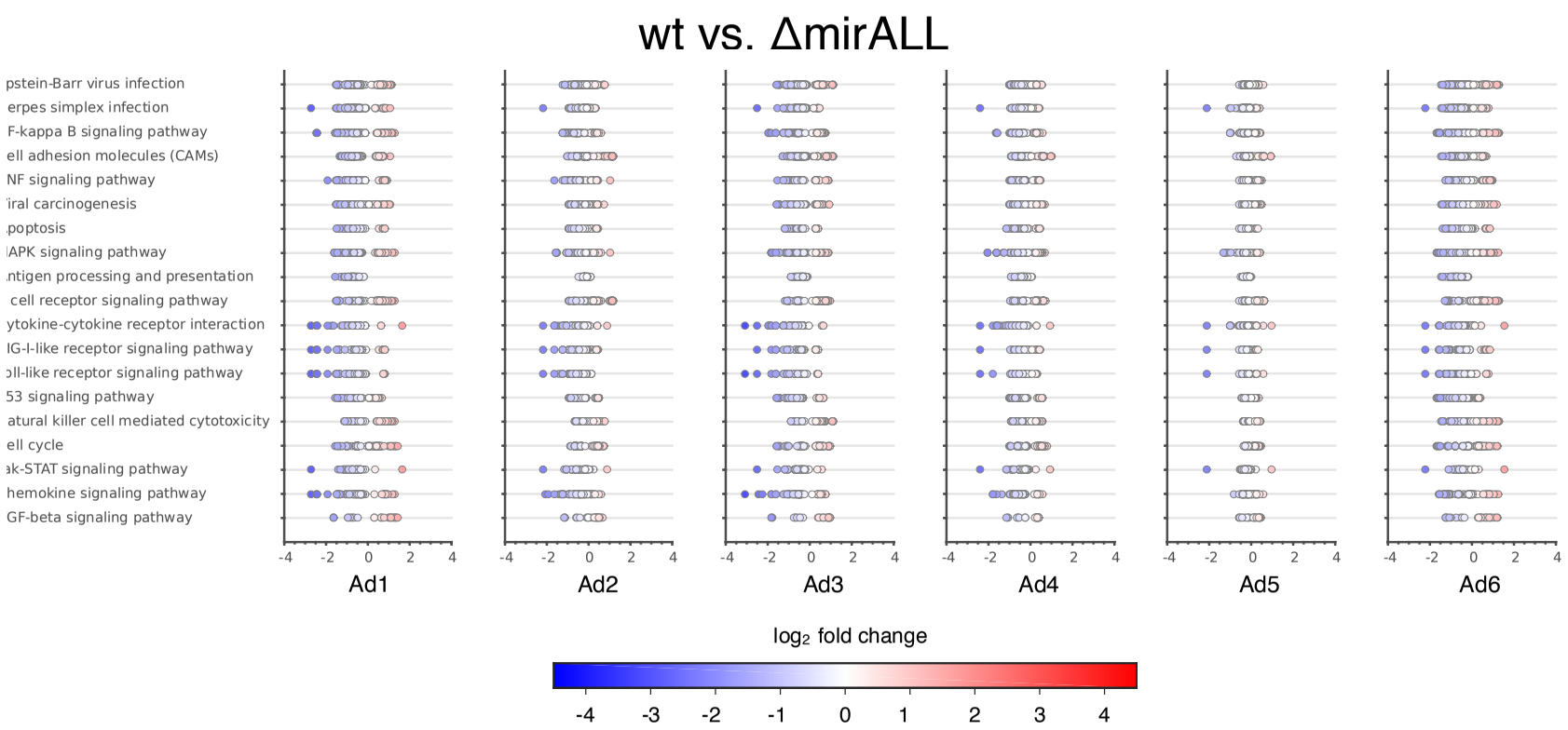

Supplementary Figure 1 KEGG pathway enrichment analysis comparing wt and ΔmirALL EBV-infected B cells

KEGG enrichment analysis of selected pathways, which are listed according to their significances in descending order. The analysis on the basis of the top differentially regulated genes comparing “wt vs. ΔmirALL” EBV-infected B cells is described as in Fig. 8A. The results for all six samples are shown.

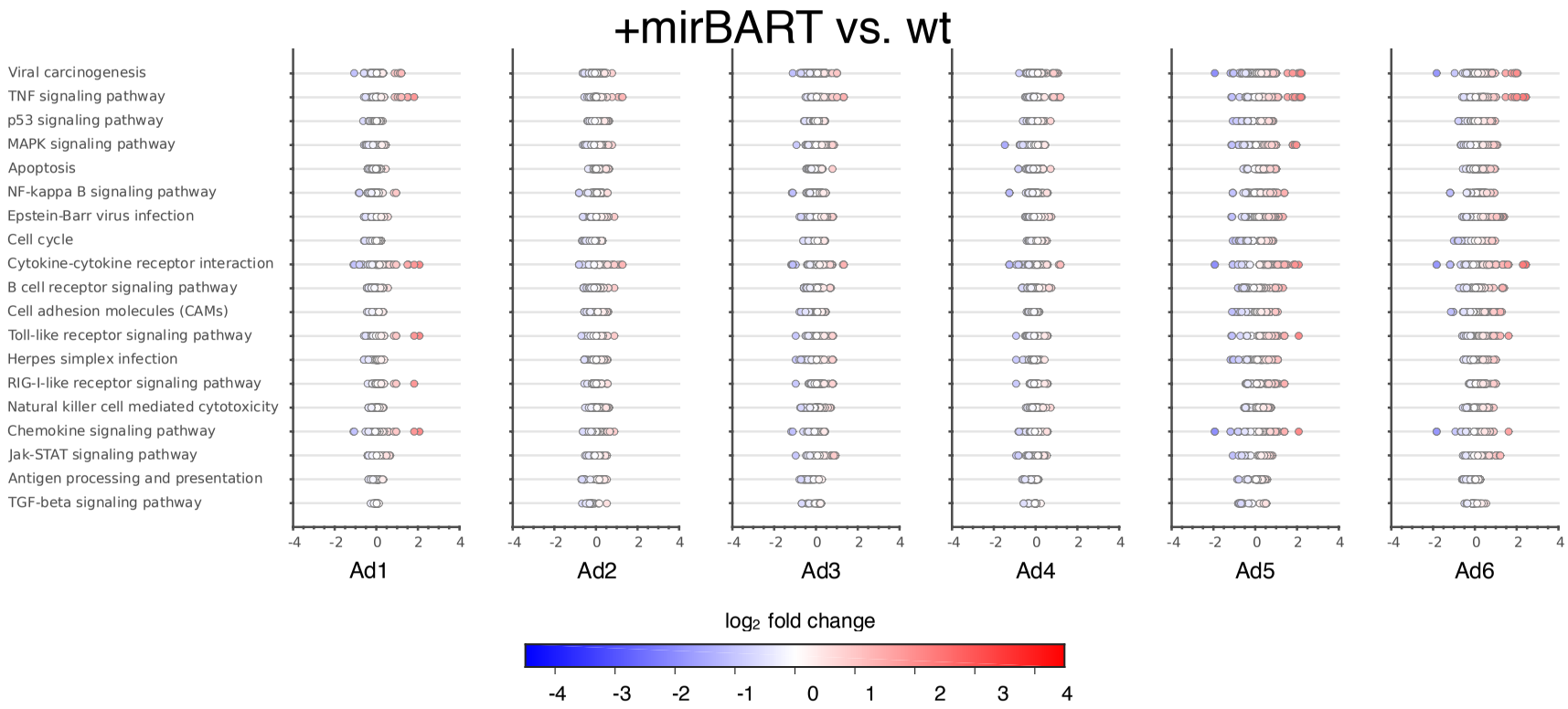

Supplementary Figure 2 KEGG pathway enrichment analysis comparing +mirBART and wt EBV-infected B cells

KEGG enrichment analysis of selected pathways, which are listed according to their significances in descending order. The analysis on the basis of the top differentially regulated genes comparing “+mirBART vs. wt” EBV-infected B cells is described as in Fig. 9A. The results for all six samples are shown.

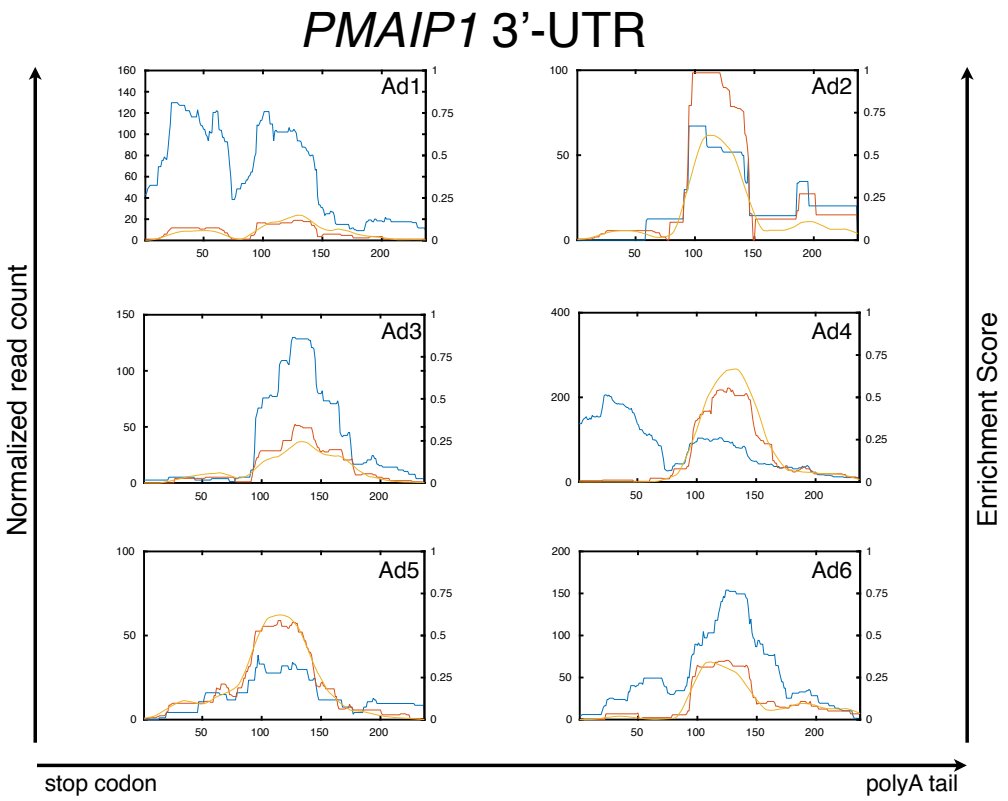

Supplementary Figure 3 AGO2 RIP-Seq analysis of *PMAIP1*

AGO2 RIP-Seq analysis of B cells infected with wt EBV or ΔmirALL EBV. EBV-infected B cells were lysed and RIP-Seq against AGO2 was performed at day five post infection. Bioinformatical analysis were performed and shown as in Fig. 11. The result for the 3-'UTR of *PMAIP* mRNA is shown. As in *IL12B* (Fig. 11), only two of six samples showed high enrichment scores.

IL12B mut (BART1)

```
target 5' AAUAUGGCUCCAUGAAGGUGCUAC 3'
           |:||:|||| ||:  |||||||
miRNA  3' CUGUAUCACC UAUCGCCACGAU  5'
           |:||:|||| ||:  |XXXX||
mut    5' AAUAUGGCUCCAUGAAG**CACG**UAC 3'
```

IL12B mut (BART2)

```
target 5' AGCAUGUUUGAACCUGAUACACAAUUAUGACCAGAAAAUAU 3'
           ||| |  :||               |||  |||||||||
miRNA  3'  CGUUCCCGCU               UAC  GUCUUUUAU  5'
           ||| |  :||               |||  |||XXXX||
mut    5' AGCAUGUUUGAACCUGAUACACAAUUAUGACCAG**UUUU**UAU 3'

target 5' GGCAGGUGGCUUCUUAACAGCCCUGUGAGAAGCAGACAGAUGCAAAGAAAAUC 3'
           |||:| |||              |             :|||||  ||||||
miRNA  3'  CGUUC CCG              C             UUACGU  CUUUUAU 5'
           |||:| |||              |             :|||||  |XXXX|
mut    5' GGCAGGUGGCUUCUUAACAGCCCUGUGAGAAGCAGACAGAUGCAAAG**UUUU**UC 3'
```

IL12B mut (BART10)

```
target 5' UCAGCUAAU       UUAUGUAU 3'
           ||||:|||       |||||||
miRNA  3' UGUCGGUUGAGGUACCAAUACAU  5'
           ||||:|||       ||XXXX|
mut    5' UCAGCUAAU       UU**UACA**AU 3'


target 5'  GGGCCUUCAUGCUAUUUAAAUAUUUAAGUAAUUUAUGUAU 3'
            :|||  |   |:||            |    |||||||
miRNA  3' UGUCGGUUGA  GGUA            CC   AAUACAU  5'
            :|||  |   |:||            |    ||XXXX|
mut    5'  GGGCCUUCAUGCUAUUUAAAUAUUUAAGUAAUUU**UACA**AU 3'
```

IL12B mut (BART22)

```
target 5'   GGCUGAACUAAUAAAAACUCUUCUUUGUAAU 3'
             :||| ||:|           ||||||||
miRNA  3' UGAUGAUCUGGUACU        GAAACAUU  5'
             :||| ||:|           ||XXXX||
mut    5'   GGCUGAACUAAUAAAAACUCUUCU**AACA**AAU 3'
```

*PMAIP1*_mut#1

```
wt:5' AUGGAAGACCCUUGAAAAUAAAGAAGUA 3'
      | ||  ||   : |||||||
miRNA CGUUCCCGCUUACGUCUUUUAU
      | ||  ||   :  XX|X||
mt:5' AUGGAAGACCCUUGUCACUAAAGAAGUA 3'
```

*PMAIP1*_mut#2

```
target 5' CUAUGG AAAACUGGAAAAUAACUUUGA 3'
           | | ||  ||  ::|||||||
miRN     CGUUCCCGCUUACGUCUUUUAU
           | | ||  ||  ::|XX|X||
mut   5'  CUAUGG AAAACUGGUCACUAACUUUGA 3'
```

Supplementary Figure 4 Mutations in the 3'-UTR reporters

Representation of mutations introduced in the 3'-UTRs in reporter vectors (see Materials & Methods). Parts of wild-type 3'-UTR or mutated 3'-UTR with complementarities of corresponding miRNAs are shown for each mutations. Several mutant 3'-UTRs contain two mutations. Complementarities are based on *in silico* prediction using RNAhybrid and classified as Watson-Click ('|'), G:U (':'), or non-matching due to mutations introduced ('X').

Supplementary Tables

The tables described below can be found in the USB flash drive accompanied with this dissertation.

Supplementary Table 1 Consistently regulated transcripts by EBV miRNAs

The list of transcripts identified to be differentially regulated in the three comparisons “wt vs. ΔmirALL”, “+mirBART vs. ΔmirALL”, and “+mirBART vs. wt” EBV-infected B cells (Fig. 7B). This list contains the Ensembl Transcript IDs of transcripts that were both down- or up-regulated, corresponding gene symbols, and $\log_2$ fold changes.

Supplementary Table 2 Top highly read-enriched 3’-UTRs by AGO2 RIP-Seq

The list of transcripts identified as candidates to be bound by EBV miRNAs encoded in the wt EBV strain. This list contains genomic positions that showed high enrichment scores (Result section 4.2), the corresponding gene symbols, and the donor numbers (Ad1 to Ad6) that fulfilled the criteria described in the Result section 4.2.

Curriculum Vitae

PERSONAL INFORMATION

Surname/ Family Name	Takanobu Tagawa
Nationality	Japan

RESEARCH EXPERIENCE

Dates	June 2011 to September 2015
Supervisor	Prof. Wolfgang Hammerschmidt
Position	Doctoral student
Place	Helmholtz Zentrum München, AGV and Ludwig-Maximilians University
Thesis title	"Functional analysis of Epstein-Barr virus microRNAs early after infection of human primary B lymphocytes"

Dates	April 2009 to March 2011
Supervisor	Prof. Hideo Iba
Position	Master student
Place	The University of Tokyo, The Institute of Medical Science
Thesis title	"Multiple microRNAs induced by *Cdx1* suppress *Cdx2* in human colorectal tumor cells"

EDUCATION

Dates	April 2005 to March 2009
Position	Bachelor student
Place	The University of Tokyo, The School of Science, Department of Biophysics and Biochemistry

Dates	April 1999 to March 2005
Place	Junior & Senior High School at Komaba, University of Tsukuba